Discontinuous Galerkin *hp*-adaptive methods for multiscale chemical reactors: quiescent reactors

C.E. Michoski † ϒ
Institute for Computational Engineering and Sciences, Department of Chemistry and Biochemistry, University of Texas at Austin, Austin, TX, 78712

J.A. Evans ⋆
Computational Science, Engineering, and Mathematics, University of Texas at Austin, Austin, TX, 78712

P.G. Schmitz ≀
NumAlg (Abelian) Consulting?, Toronto, ON, M5P 2X8

Abstract

We present a class of chemical reactor systems, modeled numerically using a fractional multistep method between the reacting and diffusing modes of the system, subsequently allowing one to utilize algebraic techniques for the resulting reactive subsystems. A mixed form discontinuous Galerkin method is presented with implicit and explicit (IMEX) timestepping strategies coupled to dioristic entropy schemes for *hp*-adaptivity of the solution, where the h and p are adapted based on an L^1-stability result. Finally we provide some numerical studies on the convergence behavior, adaptation, and asymptotics of the system applied to a pair of equilibrium problems, as well as to general three-dimensional nonlinear Lotka-Volterra chemical systems.

Keywords: Chemical reactors, reaction-diffusion equations, SSPRK, RKC, IMEX, discontinuous Galerkin, Fick's Law, energy methods, *hp*-adaptive, Lotka-Volterra, integrable systems, thermodynamics.

Contents

†*michoski@cm.utexas.edu*, ϒ Corresponding author
⋆ *evans@ices.utexas.edu*, ≀ *pschmitz@math.utexas.edu*

§1 Introduction

Broadly speaking, chemical reactor systems might be defined as: those systems arising in nature that are dominated, inherently characterized, or significantly influenced by dynamic reactions between the discernible constituents of multicomponent mixtures. These systems are of fundamental importance in a number of scientific fields [67], spanning applications in chemistry and chemical engineering [39, 47, 81], mechanical and aerospace engineering [77], atmospheric and oceanic sciences, [23, 58, 80] astronomy and plasma physics [38, 90], as well as generally in any number of biologically related fields (viz. [68] for example).

Much of the underlying theory for reactor systems may be found in the classical texts [21, 34, 47], where generally reactor systems are derived using kinetic theory by way of a Chapman–Enskog or Hilbert type perturbative expansions. These derivation processes immediately raise important theoretical concerns beyond the present scope of this paper (see [19, 84] for an example of the formal complications that may arise in rigorous treatments). Here we restrict ourselves to the study of a set of simplified systems leading to a generalizable class of reaction-diffusion equations, that may be referred to collectively as: quiescent reactors. This designation (as we will see below) is chosen in keeping with the parlance of chemical engineering and analytic chemistry, wherein quiescent reactors refer to systems that are relatively "still" in some basic sense.

The theory provides that quiescent reactor systems may be derived directly from fluid particle systems (i.e. the Boltzmann equation), wherein a number of underlying assumptions on the system must be made explicit. These derivations can become quite involved, and can vary with respect to the scope of the application. For some examples of these derivations we point the interested reader to [1, 11, 13, 28, 31, 35, 45, 51]. On the other hand, from the point of view of the experimental sciences, a quiescent reactor may be defined abstractly as a reactive chemical system wherein the effects from "stirring" are either not present, or do not play a significant role in the dynamic behavior of the medium [66]. We will make precise below our meaning of the term "quiescent" as it applies in this paper, but suffice it to say at the outset that a quiescent reactor system is one that may be approximated by a class of constrained systems of reaction-diffusion equations in the molar concentrations of the associated n chemical constituents.

A large number of numerical approaches to closely related reaction-diffusion systems exist in the literature (though often in single-component versions), some of which we discuss in the body of this paper in some detail. Let us review here briefly some results that will not be discussed in great detail below. In addition to the very important operator splitting methods in the temporal space that employ the Strang method formalism [30, 62] and its entropic structure (which we shall discuss briefly below), Petrov-Galerkin methods have been applied [49, 87]. Petrov-Galerkin-type methods offer interesting benefits in that they allow for the development of "optimal" test functions, that are modified in a trial space by utilizing properties of the solution residual itself [27]. Mesh adaptive finite volume (multiresolution) methods have also been found to work well in a number of complicated application settings [9, 72], where fixed tolerance methods are deployed for "sensing" local structure in the solution. The compact implicit integration factor (cIFF,IFF,cIFF2,ETD) methods over adaptive spatial meshes [56] have been developed, when computational efficiency concerns are of central importance, and the system is too stiff for explicit methods to be realistic. In addition, particle trajectory based methods [10] and stochastic methods have been developed [4, 37], yet these approaches might be seen as critical departures from the Eulerian frame continuum solutions of interest here.

We view our present approach as aiming towards a dynamic extension of the pioneering work in [3, 8, 64] on diffusive systems, to the *hp*-adaptive finite element reaction-diffusion systems studied in [57, 74, 88, 89]. The subsequent method that we implement can be referred to as a mixed form IMEX discontinuous Galerkin stability preserving fractional multistepping dioristic-entropic *hp*-adaptive scheme. The present approach is a high order accurate implementation that supports robust multiscale resolution both spatially (e.g. *hp*) and temporally (e.g. fractional multistepping). This is the first discontinuous Galerkin application method of its type to be

implemented, where we show optimal convergence behavior, and further address hybrid approaches to solving the difficult (and often numerically stiff) reaction subsystems in a way that provides substantial improvements to both the accuracy of the solution as well as the computational performance of the algorithm. In this work we significantly extend the heuristic p-enrichment type strategies discussed in [58] to utilize the formal entropy of the underlying system. The entropy of the system is an important physical and mathematical aspect of the fully coupled system, and is here formally derived for the system then used as an *a posteriori* variable to determine local variation of the solution. This is then worked formally into a sharp dynamic hp-adaptive strategy that couples h-refinement and coarsening strategies to p-enrichment and de-enrichment strategies by way of a kinetic switch algorithm.

In §2.1 we begin by outlining a formal physical derivation of the system of model problems with which we are concerned. In §2.2 we then explicitly denote the quiescent reactor system in terms of a coupled system of reaction-diffusion equations characterized by a highly nonlinear chemical reaction term (the law of mass action). Next, in §2.3, we cast the numerical setting that the problem will take, first the reaction term is discussed in §2.4, and in §2.5 the diffusion term is discussed. We proceed in §2.6 by developing the spatial discretization that we will use in our generalized finite element discrete form model, and in §2.7 we formulate the fully discrete system. In §3 an exact entropy relation is derived. This entropy relation, which is also a TVB and L^1–stability result, is then used to develop an hp-adaptive scheme for the coupled system of reaction–diffusion equations. Finally, in §4 we present some example applications using some of the data structures developed in [6, 7]. The first example is an simple academic test in linear equilibrium given an exact form solution, and the second case is a more complicated nonlinear example, derived in the context of a Lotka-Volterra chemical system with three constituents.

§2 Deriving the system

§2.1 The species Boltzmann equation

Let us outline a formal derivation of the reaction–diffusion equation, which will serve as the theoretical underpinning for our quiescent reactor systems. For full definitions and an expansive review of the underlying objects in this section, we point the reader in the direction of [21, 40]. For background on the derivation and a discussion of how the Boltzmann equation may be viewed as the classical limit of the quantum mechanical Waldmann-Snider equation, we direct the reader to [53].

We begin by considering the species Boltzmann equation comprised of $i = 1, \ldots, n$ species in $N = 1, 2$, or 3 spatial dimensions over $(t, \boldsymbol{x}, \boldsymbol{v}) \in (0, T) \times \Omega^2$ for $\Omega \subseteq \mathbb{R}^N$. Taking the n distribution functions f_i and the velocity of the i-th species given by $\boldsymbol{v}_i$, and assuming an absence of external forces, the species Boltzmann equation is determined by:

$$\partial_t f_i + \boldsymbol{v}_i \nabla_x f_i = \mathfrak{S}_i(f) + \mathfrak{C}_i(f). \tag{2.1}$$

Here $\mathfrak{S}_i(f)$ corresponds to nonreactive scattering and $\mathfrak{C}_i(f)$ to the reactivity of the coupled chemically reactive system.

Now consider the usual Enskog expansion of (2.1), such that to linear order we have

$$\partial_t f_i + \boldsymbol{v}_i \nabla_x f_i = \epsilon^{-1} \mathfrak{S}_i(f) + \epsilon^b \mathfrak{C}_i(f), \quad \text{and} \quad f_i = f_i^0 \left(1 + \epsilon \eta_i + \mathcal{O}(\epsilon^2)\right), \tag{2.2}$$

where ϵ is the formal expansion parameter. The perturbations η_i are used to determine the respective forms of the corresponding transport coefficients, and the parameter b distinguishes between the differing regimes of interest. When $b = 0$ then we are in the so-called strong reaction regime, when $b = 1$ we are in the Maxwellian reaction regime, and when $b = -1$ we are in the kinetic chemical equilibrium regime. Note that only in kinetic equilibrium are the scattering and reactive modes commensurate over timescales of the same order of magnitude.

§2.1.1 Cases of $b = 1$ and $b = 0$

First consider the cases $b \in \{1, 0\}$. Here note that for the zeroth order expansion, if we equate the powers of ϵ^{-1} then the distribution functions f_i^0 are found by solving $\mathfrak{S}_i(f^0) = 0$, where $f^0 = (f_1^0, \ldots, f_n^0)$. This result naturally recovers that the f_i^0 are Maxwellian distribution functions (see [21, 40] for more details on this

standard result). Moreover, we define the maximum contracted scalar product by,

$$(\zeta, \varphi)_{mcs} = \sum_{i_q=1}^{n_q} \sum_{i=1}^{n} \int_\Omega \zeta_i \odot \varphi_i d\boldsymbol{v}_i,$$

such that when either ζ_i or φ_i is a scalar, then $\zeta_i \odot \varphi_i = \zeta_i \varphi_i$. If both are vectors, then $\boldsymbol{\zeta}_i \odot \boldsymbol{\varphi}_i = \boldsymbol{\zeta}_i \cdot \boldsymbol{\varphi}_i$. And if both are matrices, then $\zeta_i \odot \varphi_i = \zeta_i : \varphi_i$. Here, the i_q index the total number of quantum internal energy states n_q in the transition probability integral representation (see [40] for more details).

Now we are interested in recovering the bulk continuum equations. As such we define the number density of the i-th constituent $\mathfrak{n}_i$ and the species mass density ρ_i respectively by

$$\mathfrak{n}_i = \sum_{i_q}^{n_q} \int_\Omega f_i d\boldsymbol{v}_i \quad \text{and} \quad \rho_i = \sum_{i_q}^{n_q} \int_\Omega \mathfrak{m}_i f_i d\boldsymbol{v}_i, \quad \text{with } \mathfrak{m}_i \in \mathbb{R} \text{ the molecular mass of species } i. \tag{2.3}$$

The momentum $\rho\boldsymbol{u}$ and the total specific energy density $\rho\mathfrak{E}$ is given in terms of the total density $\rho = \sum_i \rho_i$, the flow velocity $\boldsymbol{u}$ and the internal energy per unit volume $\mathscr{E}$, such that:

$$\rho\boldsymbol{u} = \sum_{i}^{n} \sum_{i_q}^{n_q} \int_\Omega \mathfrak{m}_i f_i \boldsymbol{v}_i d\boldsymbol{v}_i \quad \text{and} \quad \rho\mathfrak{E} = \left(\frac{\rho}{2}|\boldsymbol{u}|^2 + \mathscr{E}\right) = \sum_{i}^{n} \sum_{i_q}^{n_q} \int_\Omega \left(\frac{\mathfrak{m}_i}{2}|\boldsymbol{v}_i|^2 + \mathcal{E}_{ii_q}\right) f_i d\boldsymbol{v}_i, \tag{2.4}$$

where $\mathcal{E}_{ii_q}$ is the corresponding internal energy in the i_q-th quantum state of the i-th constituent.

Next, by using the usual $n+4$ collisional invariants ψ_ℓ of $\mathfrak{S}_i(f)$, given by

$$\begin{aligned}
\psi_\ell &= \delta_{\ell i} \quad \text{for} \quad \ell, i \in \{1, \dots, n\}, \\
\psi_{n+j} &= \mathfrak{m}_i v_{ji} \quad \text{for} \quad i \in \{1, \dots, n\}, j \in \{1, 2, 3\}, \\
\hat{\psi}_{n+4} &= \tfrac{1}{2}\mathfrak{m}_i |\boldsymbol{v}_i|^2 + \mathcal{E}_{ii_q} \quad \text{for} \quad i \in \{1, \dots, n\},
\end{aligned}$$

where $\delta_{\ell i}$ is the Kronecker symbol, we obtain by construction that,

$$(\psi_\ell, \mathfrak{S}(f))_{mcs} = \sum_{i_q=1}^{n_q} \sum_{i=1}^{n} \int_\Omega \psi_\ell \mathfrak{S}_i(f) d\boldsymbol{v}_i = 0, \quad \forall \ell \in \{1, \dots, n+4\},$$

Then taking the scalar product of (2.2) with the collisional invariants ψ_ℓ and letting δ_{b0} be the Kronecker delta, we find

$$\left(\psi_\ell, \partial_t f^0 + \boldsymbol{v}_i \nabla_x f^0\right)_{mcs} = \left(\psi_\ell, \epsilon^{-1}\mathfrak{S}(f^0) + \delta_{b0}\epsilon^b \mathfrak{C}(f^0)\right)_{mcs}, \quad \forall \ell \in \{1, \dots, n+4\}, \tag{2.5}$$

letting $\mathfrak{S}(f^0) = \left(\mathfrak{S}_1(f^0), \dots, \mathfrak{S}_n(f^0)\right)$ and $\mathfrak{C}(f^0) = \left(\mathfrak{C}_1(f^0), \dots, \mathfrak{C}_n(f^0)\right)$. Equating powers of ϵ^0 recovers:

$$\text{The species Euler equations} \quad \begin{cases} \partial_t \rho_i + \nabla_x \cdot (\rho_i \boldsymbol{u}) - \delta_{b0}\mathfrak{m}_i \mathscr{A}_i(\mathring{\mathfrak{n}}) = 0, \\ \partial_t(\rho\boldsymbol{u}) + \nabla_x \cdot (\rho\boldsymbol{u} \otimes \boldsymbol{u}) + \nabla_x \mathbb{S} = 0, \\ \partial_t(\rho\mathfrak{E}) + \nabla_x \cdot ((\rho\mathfrak{E} + p)\boldsymbol{u}) = 0. \end{cases} \tag{2.6}$$

We will define the stress tensor $\mathbb{S}$ and the chemical mass action $\mathscr{A}_i(\mathring{n})$ in some detail below. Note that the $\mathring{(\cdot)}$ notation indicates the subset of constituents in the set $\{1, \dots, n\}$ directly reacting with constituent i; or within the "reaction ring" of constituent i.

In order to recover the first order approximation, or the species Navier–Stokes equations in terms of the perturbation parameters η_i from (2.2), a decomposition into scattering and reactive perturbative components must be made, such that $\eta_i = \eta_i^{\mathfrak{S}} + \delta_{b0}\eta_i^{\mathfrak{C}}$. As we will see explicitly below for the case of the mass diffusion coefficient, this decomposition leads to a set of constrained integral equations that uniquely determine the η_i's. Defining $\eta = (\eta_1, \dots, \eta_n)$ and evaluating (2.5) keeping only terms in ϵ^0 and ϵ^1 we have

$$\left(\psi_\ell, \partial_t(f^0 + \eta f^0 + \boldsymbol{v}_i \nabla_x f^0 + \boldsymbol{v}_i \nabla_x(\eta f^0))\right)_{mcs} = \left(\psi_\ell, \mathfrak{C}(f^0) + \delta_{b0} f^0 \eta \partial_f \mathfrak{C}(f^0)\right)_{mcs}, \quad \forall \ell \in \{1, \dots, n+4\},$$

where the partial derivative is given by $\partial_f \mathfrak{C}(f^0) = (\partial_f \mathfrak{C}_1(f^0), \dots, \partial_f \mathfrak{C}_n(f^0))$. Algebraic manipulation (see [40] for details) then yields:

$$\text{The species Navier–Stokes equations} \quad \begin{cases} \partial_t \rho_i + \nabla_x \cdot (\rho_i(\boldsymbol{u} - \mathcal{V}_i)) - \delta_{b0}\mathfrak{m}_i \tilde{\mathscr{A}}_i(\mathring{\mathfrak{n}}) = 0, \\ \partial_t(\rho \boldsymbol{u}) + \nabla_x \cdot (\rho \boldsymbol{u} \otimes \boldsymbol{u}) + \nabla_x \mathbb{S} = 0, \\ \partial_t(\rho \mathfrak{E}) + \nabla_x \cdot ((\rho \mathfrak{E} + \mathbb{S})\boldsymbol{u}) + \nabla_x \cdot \mathcal{Q} = 0. \end{cases} \tag{2.7}$$

The reaction term in (2.7) is a linear combination of the mass action $\mathscr{A}_i(\mathring{\mathfrak{n}})$ (which we define in detail in §2.2) and a linearized perturbation term $\bar{\mathscr{A}}_i$, such that $\tilde{\mathscr{A}}_i(\mathring{\mathfrak{n}}) = \mathscr{A}_i(\mathring{\mathfrak{n}}) + \delta_{b0}\bar{\mathscr{A}}_i$. The perturbation term $\bar{\mathscr{A}}_i$ provides an estimate for the change in the reactivity of the chemical system with respect to the distribution function $\partial_f \mathfrak{C}(f^0)$, such that the linearization leads to a pair of partial rates. These terms are generally considered to be negligibly small [47], and as such the terms depending on the partial rates are often neglected. For simplicity we shall do so here as well, which formally means that we consider systems in the limit $\partial_f \mathfrak{C}(f^0) \to 0$.

The constitutive laws in (2.6) and (2.7) can be written as follows. Let $l = 1$ when we are in the Navier–Stokes regime and zero otherwise. Then the stress tensor is given by

$$\mathbb{S} = p\mathbb{I} - \delta_{1l}\left(\xi(\nabla_x \cdot \boldsymbol{u})\mathbb{I} + \mu\Big\{\nabla_x \boldsymbol{u} + (\nabla_x \boldsymbol{u})^\top - \frac{2}{3}(\nabla_x \cdot \boldsymbol{u})\mathbb{I}\Big\} + \delta_{b0}\pi_{ch}\mathbb{I}\right),$$

where μ is the shear viscosity coefficient, ξ is the bulk viscosity coefficient, and the chemical pressure π_{ch} is given to satisfy $\pi_{ch} = \sum_{r \in \mathfrak{R}} \mathfrak{h}_r \bar{\mathscr{A}}_r$, but because of — as discussed above — the presence of partial rates in $\bar{\mathscr{A}}_r$ this term will vanish. Finally, the species diffusion velocity $\mathcal{V}_i$ decomposes into a linear combination of the mass diffusion $p^{-1}\mathcal{D}_{ij}\partial_{\rho_i} p \nabla_x \rho_i$ and the thermal diffusion $(p^{-1}\mathcal{D}_{ij}\partial_\vartheta p_i + \vartheta^{-1}\theta_i)\nabla_x \vartheta$, where ϑ is the temperature and p_i is the partial pressure such that $\sum_i p_i = p$ is the total pressure and is assumed to satisfy the perfect gas law. Here we denote the multicomponent diffusion coefficient by $\mathcal{D}_{ij}$ and the thermal diffusion coefficient by θ_i. Then the species diffusion velocity $\mathcal{V}_i$ is defined by

$$\mathcal{V}_i = p^{-1}\mathcal{D}_{ij}\partial_{\rho_i} p \nabla_x \rho_i + (p^{-1}\mathcal{D}_{ij}\partial_\vartheta p_i + \vartheta^{-1}\theta_i)\nabla_x \vartheta. \tag{2.8}$$

We shall return to the coefficients $\mathcal{D}_{ij}$ and θ_i below.

Taking a similar form to that of the diffusion velocity, the heat flux $\mathcal{Q}$ also separates into terms depending on the spatial gradients of the temperature and species of the mixture. Here, the specific enthalpy h_i weighted diffusion component of $\mathcal{Q}$ is given by $\sum_i h_i \rho_i \mathcal{V}_i$, where $\mathcal{V}_i$ is defined as above. Fourier's law additionally provides for $\tilde{\lambda}\nabla_x \vartheta$ where $\tilde{\lambda}$ is the coefficient of heat conductivity. The third distinct term arising in the heat flux is often termed the Dufour effect and is written to satisfy $\sum_i \theta_i \nabla_x p_i$. Putting these together and rearranging some we arrive with:

$$\mathcal{Q} = \sum_{i=1}^{n} \left(\mathfrak{m}_i \mathfrak{n}_i h_i p^{-1}\mathcal{D}_{ij}\partial_{\rho_i} p - \theta_i \partial_{\rho_i} p_i\right) \nabla_x \rho_i - \left\{\tilde{\lambda} - \sum_{i=1}^{n} \left(\mathfrak{m}_i \mathfrak{n}_i h_i (p^{-1}\mathcal{D}_{ij}\partial_\vartheta p_i + \vartheta^{-1}\theta_i) - \theta_i \partial_\vartheta p_i\right)\right\} \nabla_x \vartheta. \tag{2.9}$$

In the case of kinetic chemical equilibrium, or when $b = -1$, the conservation forms that are derived (see [36]) for the Euler and Navier-Stokes regimes are formally equivalent to (2.6) and (2.7), up to the actual form the transport coefficients take. This is just to say that the basic properties of these coefficients remain unchanged (for example, both mass diffusion matrices are positive semidefinite), but the coefficients do demonstrate different quantitative behaviors depending on b. We will briefly return to this issue in §2.5.

§2.1.2 **The quiescent reactor subsystem**

The derivations in §2.1.1 and §2.1.2 show the formal asymptotics provided by the Enskog expansion of the species Boltzmann equation. We have performed the Enskog expansion in a generalized setting, allowing for inelastic binary scattering and intermolecular reactions. Given these assumptions, we are interested in restricting to a subsystem, which formally emerges whenever the following set of four approximate constraints are satisfied:

$$(1)\ \mathfrak{C}_i(f^0) \gg \partial_f \mathfrak{C}_i(f^0)\ \ \forall i, \quad (2)\ \sum_i^n \int_\Omega \boldsymbol{v}_i d\boldsymbol{v}_i \simeq 0, \quad (3)\ \nabla_x \rho_i \gg \nabla_x \vartheta\ \ \forall i, \quad (4)\ h_i \simeq p(\mathfrak{n}_i \mathfrak{m}_i \mathcal{D}_{ij})^{-1}\theta_i. \tag{2.10}$$

The first constraint (1) is a very standard assumption, frequently used even in formal settings [47], since the form of the $\partial_f \mathfrak{C}_i(f^0)$ is imprecise and the term is generally considered to be small. Of course, in the case of the zeroth order expansion (2.6), assumption (1) is not even necessary.

The second constraint (2) merely assumes that the global flow velocity averages to zero over the entire domain. It is important to note that this assumption is is made independent of the form of the collisional integral, and thus does not have any direct bearing on the diffusivities of the flow. In other words, the second constraint restricts to systems where the random collisional molecular motion of the fluid dominates the advective flow characteristic.

The third (3) and fourth (4) constraints from (2.10) end up being closely related. For the zeroth order expansion these constraints are unnecessary, where all that is required is the assumption of an isentropic Eulerian flow along with constraint (2). However, in the first order expansion the compressible barotropic regime does not preserve a constant entropy, but rather dissipates entropy [59, 61]. As a consequence we must restrict to solutions, which constrain the admissible bounds on the thermal gradients. It turns out that (4) in (2.10) is equivalent to setting a constraint on the total thermal variation of the mixture, where given a reference temperature $\vartheta^{\ominus}$ and the associated specific formation enthalpy $h_j^{\ominus}$ of the j-th species, the specific enthalpy $h_j = h_j^{\ominus} + \int_{\vartheta^{\ominus}}^{\vartheta} c_{pj}(s)ds$ shows that the variation in the constant-pressure specific heat capacity $c_{pj}(\vartheta)$ of each component is constrained. This constraint puts (relatively) tight bounds on the thermal variation supported by (4). Moreover, the spatial bound on this variation is then strengthened by constraint (3), which as a consequence, fully indicates that we are interested in thermal systems that do not demonstrate rapid spatial thermal variation, but thermal systems that may nevertheless develop large species gradients.

Then given (2.10), we arrive with a reaction-diffusion formulation, which formally yields our quiescent reactor system (2.11). That is, for the zeroth order expansion when $b \in \{-1, 0, 1\}$, we are restricted to the isentropic species Euler equations under constraint (2). In either case the mass diffusion contribution is neglected, and when $b \in \{-1, 0\}$ chemical equilibrium holds. In the case of the first order expansion all of the constraints from (2.10) apply such that when $b \in \{0, 1\}$, we arrive with a full reaction–diffusion equation as outlined in detail in §2.2. Now when in chemical equilibrium (i.e. $b \in \{-1, 0\}$) the Fick's diffusion type law is satisfied under an adapted mass diffusivity coefficient. We present this system in some detail below.

§2.2 The governing reaction–diffusion equations

Due to §2.1.2, we consider a solution over $(t, \boldsymbol{x}) \in (0, T) \times \Omega$ for $\Omega \subseteq \mathbb{R}^N$ chosen to satisfy:

$$\begin{aligned} \partial_t \rho_i - \nabla_x \cdot (\mathscr{D}_i \nabla_x \rho_i) - \mathscr{A}_i(\mathring{n}) = 0, \\ \mathscr{A}_i(\mathring{n}) = m_i \sum_{r \in \mathfrak{R}} (\nu_{ir}^b - \nu_{ir}^f) \left(k_{fr} \prod_{j=1}^{n} n_j^{\nu_{jr}^f} - k_{br} \prod_{j=1}^{n} n_j^{\nu_{jr}^b} \right), \end{aligned} \tag{2.11}$$

with initial-boundary data given by

$$\rho_i(t = 0) = \rho_{i,0}, \quad \text{and} \quad a_{1i}\rho_{i,b} + \nabla_x \rho_{i,b} \left(a_{2i} \cdot \boldsymbol{n} + a_{3i} \cdot \boldsymbol{\tau} \right) = a_{4i} \quad \text{on} \quad \partial\Omega, \tag{2.12}$$

taking arbitrary functions $a_{ji} = a_{ji}(t, \boldsymbol{x}_b)$ for $j \in \{1, 2, 3, 4\}$ restricted to the boundary, where $\boldsymbol{n}$ is the unit outward normal and $\boldsymbol{\tau}$ the unit tangent vector at the boundary $\partial\Omega$.

Here, n_i is the molar concentration of the i-th chemical constituent, which up to a scaling by Avogadro's constant N_A is just the number density $n_i = N_A \mathfrak{n}_i$. We use this convention since, as we will see below, the reaction rates are often formulated in molar units. The species are given by $\rho_i = \rho\alpha_i = m_i n_i$ where α_i is the mass fraction of the i-th species, and m_i is the molar mass of the i-th species. The $\mathscr{D}_i$ are the interspecies mass diffusivity coefficients (which will be fully addressed in §2.5).

The forward and backward stoichiometric coefficients of elementary reaction $r \in \mathbb{N}$ are given by $\nu_{ir}^f \in \mathbb{N}$ and $\nu_{ir}^b \in \mathbb{N}$, while $k_{fr}, k_{br} \in \mathbb{R}$ are the respective forward and backward reaction rates of reaction r. These terms then serve to define the mass action $\mathscr{A}_i = \mathscr{A}_i(\mathring{n})$ of the reaction from (2.11). Moreover, we denote the indexing sets $\mathscr{R}^r$ and $\mathscr{P}^r$ as the reactant and product wells $\mathscr{R}^r \subset \mathbb{N}$ and $\mathscr{P}^r \subset \mathbb{N}$ for reaction r. Then for a reaction indexed by $r \in \mathfrak{R}$, occurring in a chemical reactor $\mathfrak{R} \subset \mathbb{N}$, comprised of n distinct chemical species $\mathfrak{M}_i$ the

following system of chemical equations are satisfied,

$$\sum_{j\in\mathscr{R}^r} \nu^f_{jr}\mathfrak{M}_j \underset{k_{br}}{\overset{k_{fr}}{\rightleftharpoons}} \sum_{k\in\mathscr{P}^r} \nu^b_{kr}\mathfrak{M}_k, \quad \forall r \in \mathfrak{R}. \tag{2.13}$$

Equation (2.11) obeys a standard mass conservation principle. Since the elementary reactions are balanced the conservation of atoms in the system is an immediate consequence of (2.13). Let $\mathfrak{a}_{il}$ be the l-th atom of the i-th species $\mathfrak{M}_i$, where $l \in \mathfrak{A}^r$ is the indexing set $\mathfrak{A}^r = \{1, 2, \ldots, n_{atoms,r}\}$ of the distinct atoms present in each reaction $r \in \mathfrak{R}$. Then the total atom conservation is satisfied for every atom in every reaction

$$\sum_{i\in\mathscr{R}^r} \mathfrak{a}_{il}\nu^f_{ir} = \sum_{i\in\mathscr{P}^r} \mathfrak{a}_{il}\nu^b_{ir} \quad r \in \mathfrak{R},\ l \in \mathfrak{A}^r. \tag{2.14}$$

Since the total number of atoms is conserved, so is the total mass in each reaction,

$$\sum_{i\in\mathscr{R}^r} m_i\nu^f_{ir} = \sum_{i\in\mathscr{P}^r} m_i\nu^b_{ir} \quad \forall r \in \mathfrak{R}. \tag{2.15}$$

It then immediately follows that an integration by parts yields the following bulk conservation principle that is satisfied globally:

$$\frac{d}{dt}\sum_{i=1}^{n}\int_\Omega \rho_i dx = 0. \tag{2.16}$$

Moreover, a point that we belabor in §3, is that the system of chemical reactions are spontaneous $\Delta G \leq 0$ (up to a constant) with respect to the standard total Gibbs free reaction energy of the system, which further provides that the entropy of the system dissipates (see §3 for the details and a derivation).

Let us proceed by transforming our system of equations into the matrix representation by introducing the following n-dimensional state variables: $\boldsymbol{\rho} = (\rho_1, \ldots, \rho_n)^\top, \mathscr{D} = (\mathscr{D}_1, \ldots, \mathscr{D}_n)^\top, \mathscr{A}(\mathring{\boldsymbol{n}}) = (\mathscr{A}_1(\mathring{n}), \ldots, \mathscr{A}_n(\mathring{n}))^\top$. Moreover we define the "auxiliary variable" $\boldsymbol{\sigma}$, such that using $\mathscr{A} = \mathscr{A}(\mathring{\boldsymbol{n}})$ we may recast (2.11) as the coupled system,

$$\boldsymbol{\rho}_t - \nabla_x \cdot (\mathscr{D}\boldsymbol{\sigma}) - \mathscr{A} = 0, \quad \text{and} \quad \boldsymbol{\sigma} - \nabla_x\boldsymbol{\rho} = 0, \tag{2.17}$$

where we have denoted the spatial gradient, $\nabla_x\boldsymbol{\rho} = \sum_{i=1}^N \partial_{x_i}\boldsymbol{\rho}$.

Finally, we should note that under special circumstances the full system (2.11) admits traveling-wave solutions that model important physical features of 2.11), such as phase transitions, oscillatory chemical reactions, and action potential formation, e.g. [69, 76, 91]. The class of traveling-wave solutions allow under certain circumstances (2.11) to be transformed into a system of second order (though often still highly nonlinear) ordinary differential equations (ODEs). It should also be noted that traveling-wave solutions exist that are not merely asymptotic behavior arising in the diffusion limit [69, 76]. We will see below that the presence of solutions of this class, and singular solutions in general, have a significant impact on how one approaches developing a numerical strategy that can easily adapt to the subtleties of quiescent reactor systems.

§2.3 **The fractional multistep operator splitting**

Now we consider the multiscale solutions to (2.11) that split over "fast" $\boldsymbol{\rho}_f$ and "slow" $\boldsymbol{\rho}_s$ modes. That is, we consider (2.11) as a system that can be split into two evolution operators: (a) the diffusive subsystem (or ideally parabolic subsystem), and (b) the reaction subsystem. Each of these subsystems then decompose into fast and slow modes, so we have, for example, the fast reaction modes and the slow diffusion modes, etc. This leads to four possible modes, with each evolutionary subsystem with a fast and slow mode. However, it should be noted that splitting the modes into "fast" and "slow" is done here for simplicity of presentation only. The notion of "fast" and "slow" modes here is made to highlight a qualitative choice, where the physics of the system may, of course, be substantially more complicated. That is, for simplicity in our derivation, we have assumed that the rate laws (and diffusive time-scales) split into no more than two distinct sets of "fast" and "slow," while there may, of course, be k arbitrary such sets representing k grouped rates each of a quantitatively different order of magnitude. While in some physical systems it is essential to neglect the chemical kinetics of reactions occurring on substantially different timescales (e.g. neutrino production rates in atmospheric chemistry, etc.), in

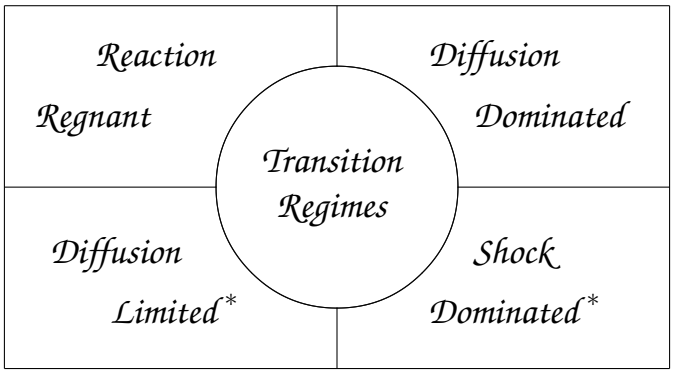

Figure 1: At any time $t \in (0, T)$ the local behavior of the solution $\boldsymbol{\rho}$ in Ω may be defined as one of the above four regimes, or are transitioning between them. Here the starred regimes $*$ denote heuristic solutions, where the transitioning regimes may or may not be heuristic depending on which regimes are being transitioned through.

many settings (such as in environmental science, for example) it is important to include reactions occurring in a number of different phases (i.e. ice, water, water vapor, etc.), which can have a large array of different timescales for their coupled rates laws. In standard units, common chemical reaction rates can differ in a particular setting up to some fifteen orders of magnitude.

Nevertheless, for simplicity we will consider the reaction such that we have only two distinct modal decompositions. We will represent this by assuming that such a system splits as $\boldsymbol{\rho} = \boldsymbol{\rho}_f + \boldsymbol{\rho}_s$, such that (2.17) may be rewritten (up to the suppressed initial-boundary data) as the coupled system:

$$\text{fast/slow splitting} \begin{cases} (\boldsymbol{\rho}_f)_t - \nabla_x \cdot (\mathscr{D}_f \boldsymbol{\sigma}_f) - \mathscr{A}_f = 0, & \text{and} \quad \boldsymbol{\sigma}_f - \nabla_x \boldsymbol{\rho}_f = 0, \\ (\boldsymbol{\rho}_s)_t - \nabla_x \cdot (\mathscr{D}_s \boldsymbol{\sigma}_s) - \mathscr{A}_s = 0, & \text{and} \quad \boldsymbol{\sigma}_s - \nabla_x \boldsymbol{\rho}_s = 0. \end{cases} \tag{2.18}$$

The "fast" and "slow" modes of the system correspond to "fast" Δt_f and "slow" Δt_s discrete timescales, often of substantially different magnitudes [30]. Also note that for notational simplicity the coupling determines the arguments of the operator, such that:

$$\mathscr{D}_f \boldsymbol{\sigma}_f = (\mathscr{D}_f \boldsymbol{\sigma}_f)(\mathscr{D}(\boldsymbol{\rho}_f)\boldsymbol{\sigma}_f, \mathscr{D}(\boldsymbol{\rho}_s)\boldsymbol{\sigma}_s) \quad \text{and} \quad \mathscr{D}_s \boldsymbol{\sigma}_s = \mathscr{D}_s \boldsymbol{\sigma}_s(\mathscr{D}(\boldsymbol{\rho}_f)\boldsymbol{\sigma}_f, \mathscr{D}(\boldsymbol{\rho}_s)\boldsymbol{\sigma}_s),$$
$$\mathscr{A}_f = \mathscr{A}_f(\boldsymbol{\rho}_f, \boldsymbol{\rho}_s) \quad \text{and} \quad \mathscr{A}_s = \mathscr{A}_s(\boldsymbol{\rho}_f, \boldsymbol{\rho}_s).$$

This notation is somewhat cumbersome, but is simply made explicit here to emphasize the fact that in this representation the modes from (2.18) are coupled by way of the nonlinear operators.

We proceed by solving (2.18) by way of a standard splitting method. That is, let us denote by $\mathcal{R}_t(\boldsymbol{\rho}_f, \boldsymbol{\rho}_s)$ the solution of the reaction part of (2.18) at time t:

$$\text{fast/slow reaction modes} \begin{cases} (\boldsymbol{\rho}_f)_t - \mathscr{A}_f = 0, \\ (\boldsymbol{\rho}_s)_t - \mathscr{A}_s = 0. \end{cases} \tag{2.19}$$

Next we denote by $\mathcal{D}_t(\boldsymbol{\rho}_f, \boldsymbol{\rho}_s)$ the solution of the diffusion part of (2.18) at time t:

$$\text{fast/slow diffusion modes} \begin{cases} (\boldsymbol{\rho}_f)_t - \nabla_x \cdot (\mathscr{D}_f \boldsymbol{\sigma}_f) = 0, & \text{with} \quad \boldsymbol{\sigma}_f - \nabla_x \boldsymbol{\rho}_f = 0, \\ (\boldsymbol{\rho}_s)_t - \nabla_x \cdot (\mathscr{D}_s \boldsymbol{\sigma}_s) = 0, & \text{with} \quad \boldsymbol{\sigma}_s - \nabla_x \boldsymbol{\rho}_s = 0. \end{cases} \tag{2.20}$$

Then with respect to our splitting (2.18), we may determine the splitting order accuracy of our desired solution simply by choosing the appropriate splitting scheme. For example, the first order accurate Lie, or sequential, splitting determines that at time t we solve either $L^t_{\mathcal{RD}} = \mathcal{R}_t(\boldsymbol{\rho}_f, \boldsymbol{\rho}_s) \circ \mathcal{D}_t(\boldsymbol{\rho}_f, \boldsymbol{\rho}_s)$, or $L^t_{\mathcal{DR}} = \mathcal{D}_t(\boldsymbol{\rho}_f, \boldsymbol{\rho}_s) \circ \mathcal{R}_t(\boldsymbol{\rho}_f, \boldsymbol{\rho}_s)$, while the second order accurate Strang splitting determines that at time t we solve either $S^t_{\mathcal{RD}} = \mathcal{R}_{t/2}(\boldsymbol{\rho}_f, \boldsymbol{\rho}_s) \circ \mathcal{D}_t(\boldsymbol{\rho}_f, \boldsymbol{\rho}_s) \circ \mathcal{R}_{t/2}(\boldsymbol{\rho}_f, \boldsymbol{\rho}_s)$, or $S^t_{\mathcal{DR}} = \mathcal{D}_{t/2}(\boldsymbol{\rho}_f, \boldsymbol{\rho}_s) \circ \mathcal{R}_t(\boldsymbol{\rho}_f, \boldsymbol{\rho}_s) \circ \mathcal{D}_{t/2}(\boldsymbol{\rho}_f, \boldsymbol{\rho}_s)$, and so forth.

Note that the operation of composition here is given in the natural way, such that $\mathcal{D}_{t/2}(\boldsymbol{\rho}) \circ \mathcal{R}_t(\boldsymbol{\rho}) \circ \mathcal{D}_{t/2}(\boldsymbol{\rho})$

means we solve the system:

$$
\begin{aligned}
&(\boldsymbol{\rho}^*)_t - \nabla_x \cdot (\mathscr{D}\boldsymbol{\sigma}^*) = 0, \quad \boldsymbol{\rho}^*(0) = \boldsymbol{\rho}_0 \quad \text{on } [0, t/2] \\
&(\boldsymbol{\rho}^{**})_t - \mathscr{A}^{**} = 0, \quad \boldsymbol{\rho}^{**}(0) = \boldsymbol{\rho}_0^* \quad \text{on } [0, t], \\
&(\boldsymbol{\rho}^{***})_t - \nabla_x \cdot (\mathscr{D}\boldsymbol{\sigma}^{***}) = 0, \quad \boldsymbol{\rho}^{***}(0) = \boldsymbol{\rho}_0^{**} \quad \text{on } [0, t/2],
\end{aligned}
$$

where the solution to the composition is then given by $\boldsymbol{\rho}^{***}(t/2) = \boldsymbol{\rho}^{***}(t/2, \boldsymbol{x})$. Moreover, if we perform this operation over the discrete slow timestep $\Delta t^{n_s} = t^{n_s+1} - t^{n_s}$ and the discrete fast timestep $\Delta t^{n_f} = t^{n_f+1} - t^{n_f}$, then for the Strang splitting $S^{t^{n_s}}_{\mathcal{DR}}$ we write in the operator notation that: $\boldsymbol{\rho}^{n_s+1} = \mathcal{D}_{t^{n_s}/2}(\boldsymbol{\rho}^{n_f}) \circ \mathcal{R}_{t^{n_s}}(\boldsymbol{\rho}^{n_s}) \circ \mathcal{D}_{t^{n_s}/2}(\boldsymbol{\rho}^{n_f})$, where $\boldsymbol{\rho}^* = \mathcal{D}_{t^{n_s}/2}(\boldsymbol{\rho}^{n_f})$, $\boldsymbol{\rho}^{**} = \mathcal{R}_{t^{n_s}}(\boldsymbol{\rho}^*)$, and $\boldsymbol{\rho}^{***} = \mathcal{D}_{t^{n_s}/2}(\boldsymbol{\rho}^{**})$.

We shall revisit the splitting scheme in the context of the fully (temporally and spatially) discrete solution in §2.7 below. Nevertheless, as in [30], a simplification of the full splitting often arises in which we are only interested in the time order of the slowest modes of the system. In such cases it is customary to relax the time order of the fast components and rather only solve the reduced systems, given either by $S^t_{\mathcal{RD}} = \mathcal{R}_{t/2}(\boldsymbol{\rho}_s) \circ \mathcal{D}_t(\boldsymbol{\rho}_f, \boldsymbol{\rho}_s) \circ \mathcal{R}_{t/2}(\boldsymbol{\rho}_s)$ or $S^t_{\mathcal{DR}} = \mathcal{D}_{t/2}(\boldsymbol{\rho}_f, \boldsymbol{\rho}_s) \circ \mathcal{R}_t(\boldsymbol{\rho}_s) \circ \mathcal{D}_{t/2}(\boldsymbol{\rho}_f, \boldsymbol{\rho}_s)$, though we will not utilize these simplifications below. Also, it is important to note that in the Strang theory the operators $S^t_{\mathcal{RD}}$ and $S^t_{\mathcal{DR}}$ are theoretically equivalent up to second order [79]. Moreover, it is possible to sequentially raise the time order accuracy of the splitting scheme [82], though this leads to the addition of negative time coefficients (in contrast to the $t/2$ arising in the second order Strang method), requiring in the discrete method that the solution from some number of previous timesteps must be stored for future use. Thus, we will define the general splitting operator $\mathfrak{Y}^{\mathfrak{T}} = \mathfrak{Y}^{\mathfrak{T}}(\mathcal{D}, \mathcal{R}, t)$ of time order accuracy $\mathfrak{T}$ by, $\mathfrak{Y}^{\mathfrak{T}} = (L^t_{\mathcal{RD}}|_{\mathfrak{T}=1}) \vee (L^t_{\mathcal{DR}}|_{\mathfrak{T}=1}) \vee (S^t_{\mathcal{RD}}|_{\mathfrak{T}=2}) \vee (S^t_{\mathcal{DR}}|_{\mathfrak{T}=2}) \vee \ldots$, where $\vee$ denotes the logical disjunction operator (e.g. the logical "or" operator). Note that analysis in [30, 78] has shown that ending the splitting method with the "stiff" mode reduces the splitting error of the scheme, and is essential.

Let us make a few comments about the theoretical implication of the multiscale splitting (2.18). As shown in §2.1, the formal derivation of (2.11) only satisfies the appropriate asymptotics when the reaction is "slow" with respect to the diffusion. We shall refer to areas of the domain that satisfy these dynamics as diffusion dominated areas. If we dynamically adapt the diffusivity coefficient $\mathscr{D}_i$, then we may also recover the kinetic equilibrium conservation equation §2.1.2, and we will refer to areas of the domain obeying these dynamics as being reaction regnant areas (e.g. secondary geminate recombination reactions in transient species).

In biological applications another case frequently emerges where the rate of the reaction can be much faster than the rate of the diffusion locally, which is just to say that the reaction can take place "instantly" given the proper local conditions (e.g. primary geminate recombination reactions in transient species). The reaction term then acts like a switch, and the diffusion limits the dynamics of the system. These systems are not readily attainable via the Boltzmann formalism from §2.1 and are characterized by those that work on them as still being largely heuristic [52]. Moreover, they are frequently obtained by using a very different set of underlying assumptions [4, 50, 92]. Nevertheless, the (possibly incorrectly balanced) continuum form of the equation is formally equivalent to (2.11), and since our numerics easily accommodate for these systems, we will refer to areas of the domain satisfying these dynamics as diffusion limited areas as in Figure 1, and denote them as heuristic by $*$.

Finally, when the reactions fully dominate the diffusion in that the rates of the reactions are globally of a substantially faster timescale than the diffusion rates, then the system is shock dominated as in Figure 1. Since such reactions are frequently replete with large thermal gradients, catalytic volume expansions, and are generally convection dominated, we view these subsystems — insofar as they are numerically well accommodated for ("robust") in our formulation, especially when employing flux-limiting type strategies similar to [60] — as heuristic $*$ as well.

Given (2.18) all areas of the domain are either in one of the aforementioned states, or are transitioning between them at any time t (as denoted in Figure 1). This follows simply from the following two facts: (1) that the diffusion rate and reaction rates either scale, or one is larger than the other, and (2) that the reaction may run to completion leading to rate limiting constituents locally.

§2.4 **Law of mass action**

The law of mass action $\mathscr{A} = \mathscr{A}(\mathring{\boldsymbol{n}})$ may be viewed as the source of a nontrivial set of technical complications. Not only is it well known that $\mathscr{A}$ may cause numerical instabilities due to the presence of multiple characteristic

timescales in the solution space, but more so, the existence of nonlinearities that develop in the exponents of the n molar concentrations n_i's (as determined by the stoichiometric coefficients ν_{ir}^f and ν_{ir}^b) generate an n-coupled system of first order autonomous nonlinear ordinary differential equations (nFANODEs), despite the simplifying assumption of the splitting (2.19) that decouples this component from the nonlinear diffusion.

Solutions to this class of problems are fairly well-established from a purely numerical point of view, where the choice often becomes rather: which approximation scheme should be used and to what order of accuracy? However, the case of nFANODEs also makes the mass action functional $\mathscr{A}$ notable in that the decoupled system (2.19) is, relatively speaking, also "reasonably" simple to solve from some "exact" mathematical point of view (we will work to make this statement precise below). As such, developing a solution technique to equation (2.19) generally rests somewhere between: (1) finding a relatively straightforward approximate solution to (2.19), and (2) analytically solving the difficult (though often soluble) system of nFANODEs.

This section is devoted to characterizing these two distinct principal strategies for solving (2.19). The first strategy we address are "exact strategies," by which we mean solutions that have accessible analytic forms for their solutions (though these forms need not necessarily be nonsingular expressions, as discussed in detail below). We will refer to solutions developed under this premise as solutions to fully coupled strategies. The second class of strategy we address are solutions in which analytic forms for the solution are not readily computable. These solutions are recovered by way of approximate strategies.

Since both classes of strategies will be situated with respect to a variational form of (2.11), it is natural to concern ourselves with the coupled integrated rate laws for our split set of rate equations (2.19), where we define an integrated rate law as the solution to an integrable system of nFANODEs. However, the basic mathematical preliminaries deem that systems of nFANODEs need not be integrable. In particular, some elementary chemical systems $\mathfrak{R}$ characterized by the coupled rate equations (2.13) do not admit a fully coupled solution in the form of an integrated rate law, or are non-integrable systems of nFANODEs. An easily accessible example of such is when (2.19) forms a Lotka-Volterra system. Here, it is well-known that when $n = 3$ such a system admits generically many non-integrable homogeneous polynomial vector fields [63]. On the other hand, when the Lotka-Volterra system is integrable, then the homogeneous polynomial vector field characterizes a foliation whose leaves are homogeneous surfaces in the $n = 3$ dimensional space containing functions called first integrals, which completely determine the solution of the system. We will revisit the Lotka-Volterra system in §4 in some detail.

First, let us clarify our notation. Here and below let the solution space of the nFANODE determined by (2.19) be denoted $\mathfrak{G} = \mathfrak{G}(\mathring{\boldsymbol{n}})$. Next, the confluence of solutions occurs over the field $\mathbb{K}$ (where $\mathbb{K}$ is either $\mathbb{R}$ or $\mathbb{C}$), which should serve to remind the reader of the fundamental theorem of algebra (i.e. the only analytic solutions to the system may require a standard field extension to $\mathbb{C}$ even if the system of study is observed over $\mathbb{R}$). Recall then that to (2.19) there corresponds an abstract vector field, which can be written as:

$$\delta_{\mathscr{A}} = \sum_{i=1}^{n} \mathscr{A}_i \frac{\partial}{\partial n_i} = \mathscr{A} \cdot \nabla_{\mathring{\boldsymbol{n}}}.$$

The observation is that for functions of $\mathring{\boldsymbol{n}}$, such as $G : \mathbb{R}^n \to \mathbb{R}$ where $\mathring{\boldsymbol{n}} \mapsto G(\mathring{\boldsymbol{n}})$, the total time derivative is given by, $\frac{dG}{dt} = \mathscr{A} \cdot \nabla_{\mathring{\boldsymbol{n}}} G$, which is just the derivative along the flow following the solution of the nFANODE. Then a first integral of $\mathfrak{G}$ is defined as a C^1 function on a subinterval $T_{loc} \subset (0, T)$ of a local neighborhood $U \subset \mathbb{K}^n$, such that $I = I(\mathring{\boldsymbol{n}}) : T_{loc} \times U \to \mathbb{R}$ remains constant along solutions,

$$\frac{dI}{dt} = \partial_t I + \mathscr{A} \cdot \nabla_{\mathring{\boldsymbol{n}}} I = 0. \tag{2.21}$$

Clearly by scalar transport such a condition holds if and only if I is constant along all solutions $\mathring{\boldsymbol{n}}$ in $\mathfrak{G}$. Thus it is often customary to recast (2.21) as the sum of differential one-forms,

$$dI = I_t dt + I_{n_1} dn_1 + \ldots + I_{n_n} dn_n = 0, \quad \text{where} \quad I_{n_i} = \left(\frac{\partial I}{\partial n_i} \right). \tag{2.22}$$

Note that (2.21) is also admissible when I has no dependence on time, i.e. $I_t = 0$.

The basic confusion that must be preemptively dispelled is, what exactly we mean here by the notion of "integrability?" Tautologically, of course, what we mean in the context of quiescent reactor systems by

"integrable" is the formal existence of an integrated rate law for any particular instance of (2.19). Being self-referential this definition is not particularly enlightening, so let us proceed by developing a sense of the different meanings of integrability that we are concerned with here.

First we proceed by defining two notions of global integrability, when the first integrals of $\mathscr{A}$ are defined over $(0,T)\times\Omega$. In this global setting the first notion we address is that of liouvillian integrability. When (2.19) is a classical system and can be posited in terms of Hamilton's equations, then this is the notion of integrability that naturally arises.

Definition 2.1. *When the system $\mathfrak{G}$ is Hamiltonian, it is Liouville integrable if it possesses n functionally independent first integrals in involution, i.e. their mutual Poisson brackets vanish, $\{I_i, I_j\} = 0$.*

This notion of integrability represents both a verdant and mature field in classical mathematics as well as mathematical and theoretical physics. There are many approaches developing solutions to these types of problems in the literature. A particularly beautiful one, for example, involves the identification of the particular systems Lax pair. The extraordinary thing about this, is that the Lax pair of matrices along with a complex-valued "spectral" parameter $\lambda\in\mathbb{C}$ provides an isospectral (i.e. the eigenvalues remain constant in time) evolution equation, such that the characteristic equation for the eigenvalues of the Lax matrix determine the so-called spectral curve (an algebraic curve) — which is nothing more than a Riemann surface whose moduli contain the specified first integrals.

More generally, a notable feature of liouvillian integrability is how weak the condition is that it prescribes on the ramification locus of, for example, its associated algebraic variety. That is, for a system with n degrees of freedom liouvillian integrability requires only n single-valued first integrals, while the remaining canonical one-forms may correspond to non-algebraic multivalued integrals. However, when the level manifolds M_f (see [5]) generated by the intersection of the level sets of the I_i (i.e. $\cap_i I_i = c_i$) are connected and compact, then the M_f's are real topological tori and the singular points become well-behaved in a formal sense. Systems such as these are indeed replete with beautiful mathematics, become extremely subtle, and frequently require quite delicate analysis [5].

Here however, we are more generally interested in solutions that can readily be made "algorithmic," since the class of equations covered by $\mathscr{A}$ is so large. From the point of view of solving (2.19), this can be viewed as a basic limitation of the Lax pair formulation, as there is at present no general algorithm for determining the Lax pair of a particular differential system of nFANODEs.

Nevertheless, there is an algorithmic approach to finding solutions that are Liouville integrable. Such methods can be traced to Sophus Lie, who discovered in the nineteenth century that one can readily reduce the order of an nFANODE by way of applying a canonical set of group transformations along symmetries of the solution, where a "symmetry" is defined as a transformation mapping any one solution of the system to another [12, 48, 65]. Many popular algebraic methods for finding solutions to differential equations are based on these group homomorphism techniques (for example see DEtools in Maple 15), though the major drawback of each is that determining the symmetries of the system can only be done heuristically, and as such cannot guarantee that if such a symmetry exists it will in fact be found.

Moreover, the admissible forms of the canonical variables in the Liouville integrability sense has, from the point of view of singularity analysis, led to a stronger form of global integrability that is more well-behaved, known as algebraic integrability.

Definition 2.2. *The system $\mathfrak{G}$ is algebraically integrable if there exists k independent first integrals such that $I_i = C_i$ $(i = 1,\dots,k)$ are algebraic functions. These k first integrals define an $(n-k)$-dimensional algebraic variety. Additionally, there must exist $(n-1-k)$ independent first integrals given by the integral of a total differential defined on the algebraic variety*

$$F_i = \sum_{j=1}^{n-k}\int^{n_j}\psi_{ik}(\mathring{\boldsymbol{n}})dn_j,\quad i=1,\dots,n-1-k,$$

where the $\psi_{ij}(\mathring{\boldsymbol{n}})$ are algebraic functions of $\mathring{\boldsymbol{n}}$.

Notice that when $k=(n-1)$ nothing is known *a priori* about the total differential of the system, and the definition of algebraic integrability become synonymous with the existence of $n-1$ independent algebraic first integrals I_j.

It turns out that a substantial amount is known about these systems, which is largely due to their close relationship to the weak Painlevé property [42]. For example, it is known that all solutions to algebraically integrable systems can be expanded in a Puiseux series about the movable singularities t^* of $\mathfrak{G}$, such that every solution satisfies:

$$\mathring{\boldsymbol{n}} = (t - t^*)^{\boldsymbol{p}} \left(\mathbf{g} + \sum_{i=0}^{\infty} \boldsymbol{c}_i (t - t^*)^{i/s} \right)$$

where $\mathbf{g} \in \mathbb{C}^n$ and $\boldsymbol{p} \in \mathbb{Q}^n$ comprise the so-called balance $\mathcal{F} = \{\mathbf{g}, \boldsymbol{p}\}$ of the weight–homogeneous decomposition of $\mathscr{A}$, with $\boldsymbol{c}_i \in \mathbb{C}^n$ polynomials in $\ln(t - t^*)$ and $s \in \mathbb{N}$ constituting the lowest common denominator of a system-dependent set, depending on the Kovalevskaya exponents of the system and the balance $\mathcal{F}$.

These (algebraic and liouvillian) notions of global integrability are both powerful results, each accompanied with a substantial set of tools by which to analyze the nature of a given solution (see for example [5, 42] for more details). However, when solving an abstract nFANODE such as (2.19), it turns out that in general both notions are too strong to provide generalizable solution techniques within the framework of the variational problem of our discontinuous Galerkin setting. That is, relatively speaking, over all n very few solutions of physical interest exist when the law of mass action $\mathscr{A}$ admits a globally integrable solution as defined above. Consequently we utilize the following weaker notion of local integrability.

Theorem 2.3. *(A. Goriely, see [42] for the proof) Let $\mathscr{A}$ be C^0 on an open subset $V \subset (0,T) \times U$. If the initial value problem (2.19) with $\mathring{\boldsymbol{n}}_{|t=t_0} = \mathring{\boldsymbol{n}}_0$ has a unique C^1 solution, then the vector field $\delta_{\mathscr{A}}$ has n independent first integrals $\boldsymbol{I} = (I_1, \ldots, I_n)$ of class C^1 in the neighborhood of a point $(t_0, \mathring{\boldsymbol{n}}_0)$, and conversely, given n time-independent first integrals $\boldsymbol{I}$ of $\delta_{\mathscr{A}}$ of class C^1 on an open subset $V \subset (0,T) \times U$, then there exists a solution $\mathring{\boldsymbol{n}}$ of (2.19) for any constant value of $\boldsymbol{I}$.*

Given this theorem, the problem immediately becomes that of finding the n-independent first integrals $\boldsymbol{I} = (I_1, \ldots, I_n)$, and thus the local solution. It turns out that due largely to an extraordinary theorem by Prelle and Singer, a rather substantially large class of first integrals can be computed purely algorithmically. That is, if (2.19) admits a first integral that is *elementary* (*i.e.* a *first integral* made up of elementary functions), then Prelle and Singer proved that there exist m algebraic functions w_i such that the elementary first integral is logarithmic and satisfies: $w_0(\mathring{\boldsymbol{n}}) + \sum_i^m d_i \ln w_i(\mathring{\boldsymbol{n}}) = 0$.

This fact led Prelle and Singer to develop a semidecision algorithm for finding these elementary first integrals [70]. We utilize an adapted version of the extended modified Prelle–Singer algorithm from [20], which includes — in addition to elementary first integrals — a subset of liouvillian functions. Generally the algorithm works for any rational function, but we restrict naturally to the mass action $\mathscr{A}_i$ polynomial. The algorithm [42] is semidecidable [22, 32], is in itself a powerful tool for solving (2.19) in the sense of Theorem 2.3, and in simplified forms can even be found in readily available algebraic software packages [33]. The algorithm may also be computed by hand. We will analyze such a result in §4.

The above serves now to provide a definition for the first of the two principal strategies we employ to solve (2.19), namely the fully coupled strategies. Within this class we identify the following three types of solutions: (1) we say we have a fully coupled algebraic mass action solution if (2.19) is algebraically integrable, (2) we say we have a fully coupled liouvillian mass action solution if (2.19) is Liouville integrable, and (3) due to the important aspects discussed in detail in [42], we say we have a fully coupled local mass action solution if (2.19) is locally integrable and has a solution by way of the Prelle-Singer type algorithm.

We also implement a purely approximate form for the mass action functional $\mathscr{A}$. That is, as an alternative to the analytic "coupled" strategies above, we implement an approximate strategy wherein the global coupling of the system is made fully approximate. We will achieve this by way of both implicit and explicit discontinuous Galerkin schemes, as discussed in detail below in §2.6–§2.7, wherein the numerical stability of the scheme will introduce the primary challenge.

§2.5 Mass diffusivity

In the fractional operator form, the mass diffusivity equation (2.20) obeys Fick's second law of diffusion, where we are frequently restricted to variational solutions in the sense of parabolic equations (when an exact form cannot be explicitly derived, as discussed in §2.1). The auxiliary representation,

$$\boldsymbol{\rho}_t = \nabla_x \cdot (\mathscr{D}\boldsymbol{\sigma}), \quad \text{and} \quad \boldsymbol{\sigma} = \nabla_x \boldsymbol{\rho}, \tag{2.23}$$

is chosen in order to exploit the unified framework from [2, 3] by way of the flux formulation presented below. However, first let us briefly address the form of the diffusivity coefficients $\mathscr{D}$.

As is clear from §2.1 and §2.2, the diffusivity coefficient that comes into play in the quiescent reactor regime is taken formally to satisfy

$$\mathscr{D}_i = \rho_i p^{-1} \mathcal{D}_{ij} \partial_{\rho_i} p. \tag{2.24}$$

Provided the corresponding state equation for the system, the difficulty that arises in this definition is found in determining the form of the diffusivity matrix $\mathcal{D}_{ij}$.

The determination of the transport coefficients in the kinetic formulation emerges by solving the linearized variational problem in the Enskog expansion (2.2) as in §2.1. In order to complete this development the associated perturbation coefficients η_i are expanded such that:

$$\eta_i = \eta_i^{\mu} \colon \nabla_x \boldsymbol{u} - \frac{1}{3}\eta_i^{\xi} \nabla_x \cdot \boldsymbol{u} - \sum_{\ell=1}^{n} \boldsymbol{\eta}_i^{\mathcal{D}_\ell} \cdot \nabla_x p_\ell - \boldsymbol{\eta}_i^{\tilde{\lambda}} \cdot \nabla_x (1/k_b \bar{\vartheta}), \tag{2.25}$$

where η_i^{μ} is a traceless symmetric matrix, $\boldsymbol{\eta}_i^{\mathcal{D}_i}$ and $\boldsymbol{\eta}_i^{\tilde{\lambda}}$ are vector valued, and η_i^{ξ} is a scalar valued function.

Similarly we have the function Ψ_i, which is just a scaled decomposition of the left hand side of (2.1). Evaluating the i-th component yields:

$$\Psi_i = \Psi_i^{\mu} \colon \nabla_x \boldsymbol{u} - \tfrac{1}{3}\Psi_i^{\xi} \nabla_x \cdot \boldsymbol{u} - \sum_{\ell=1}^{n} \boldsymbol{\Psi}_i^{\mathcal{D}_i} \cdot \nabla_x p_\ell - \boldsymbol{\Psi}_i^{\tilde{\lambda}} \cdot \nabla_x (1/k_b \bar{\vartheta}),$$

where appropriately we have a matrix, two vectors and a scalar. Here the components are fully determined, in particular the vector component associated to the mass diffusion $\boldsymbol{\Psi}_i^{\mathcal{D}_\ell}$ takes the form $\boldsymbol{\Psi}_i^{\mathcal{D}_\ell} = \boldsymbol{c}_i(\delta_{i\ell} - \alpha_i)/p_i$, where the relative velocity $\boldsymbol{c}_i$ is given by $\boldsymbol{c}_i = \boldsymbol{v}_i - \boldsymbol{u}$.

Then, restricting to the case of the diffusion matrix, the components of the linear expansion satisfy the matrix equation

$$\mathfrak{F}(\eta^{\mathcal{D}_i}) = \Psi^{\mathcal{D}_i}, \quad \text{with constraints } \left(\eta^{\mathcal{D}_i}, \mathcal{T}\hat{\psi}_\ell\right)_{mcs} = 0, \quad \forall \ell \in \{1, \dots, n+4\}. \tag{2.26}$$

Here $\mathfrak{F}(\eta^{\mathcal{D}_i})$ corresponds to the linearized form of the right hand side of (2.1), while the $\eta^{\mathcal{D}_i}$ matrix corresponds to $\eta^{\mathcal{D}_i} = (\boldsymbol{\eta}_1^{\mathcal{D}_1}, \dots, \boldsymbol{\eta}_n^{\mathcal{D}_n})$ and $\mathcal{T}$ the canonical basis. It should be noted that in the full system the linearized decomposition has a component that corresponds to each of the coefficient η's in (2.25). Also, in contrast to the standard collisional invariants in §2.1.1, here the $\hat{\psi}_\ell$ in the $n+4$ scalar constraints of (2.26) are the modified invariants given by:

$$\begin{aligned}
\hat{\psi}_\ell &= \delta_{\ell i} \quad \text{for} \quad \ell, i \in \{1, \dots, n\}, \\
\hat{\psi}_{n+j} &= \mathfrak{m}_i \boldsymbol{c}_i \quad \text{for} \quad i \in \{1, \dots, n\}, j \in \{1, 2, 3\}, \\
\hat{\psi}_{n+4} &= \tfrac{3}{2} - |\boldsymbol{c}_i|^2 + \bar{\mathcal{E}}_i - \mathcal{E}_{ii_q} \quad \text{for} \quad i \in \{1, \dots, n\},
\end{aligned}$$

where $|\boldsymbol{c}_i|^2 = \boldsymbol{c}_i \cdot \boldsymbol{c}_i$,

$$\bar{\mathcal{E}}_i = \sum_{i_q=1}^{n_q} p_{ii_q} \mathcal{E}_{ii_q} \exp\left(-\tfrac{\mathcal{E}_{ii_q}}{k_b \vartheta}\right) \left(\sum_{i_q=1}^{n_q} d_{ii_q} \exp\left(-\tfrac{\mathcal{E}_{ii_q}}{k_b \vartheta}\right) \right)^{-1},$$

and d_{ii_q} is the degeneracy of the i_q-th quantum energy shell of the i-th species.

Then performing the variational procedure in $\eta^{\mathcal{D}_i}$ yields,

$$\left(\mathfrak{F}(\eta^{\mathcal{D}_i}), \eta^{\mathcal{D}_j}\right)_{mcs} = \left(\Psi^{\mathcal{D}_i}, \eta^{\mathcal{D}_j}\right)_{mcs}, \tag{2.27}$$

where the left hand side is given to satisfy the bracket commutator $\left(\mathfrak{F}(\eta^{\mathcal{D}_i}), \eta^{\mathcal{D}_j}\right)_{mcs} = [\eta^{\mathcal{D}_i}, \eta^{\mathcal{D}_j}]$, given explicitly in equation 2.1.29 of [35].

The variational basis ϕ is chosen as linear combinations of products of Laguerre and Sonine polynomials $S^c_{a+1/2}$ with Wang Chang–Uhlenbeck polynomials W^d_j, denoted componentwise by

$$\phi_{a0cdj} = \phi_{sj} = \left(S^c_{a+1/2}\left(\tfrac{\mathfrak{m}_j}{2k_b\vartheta}\right) |\boldsymbol{c}_j|^2 W^d_j\left(\tfrac{\mathcal{E}_{ji_q}}{k_b\vartheta}\right) \widehat{\otimes^a \tilde{\boldsymbol{c}}_j} \delta_{ji} \right) \quad i \in \{1, \dots, n\}, \text{ where } \tilde{\boldsymbol{c}}_j = \sqrt{\mathfrak{m}_j/2k_b\vartheta}\boldsymbol{c}_j$$

and $\widehat{\otimes^a \tilde{\boldsymbol{c}}_j}$ is a tensor of rank a defined by $\widehat{\otimes^0 \tilde{\boldsymbol{c}}_j} = 1$, $\widehat{\otimes^1 \tilde{\boldsymbol{c}}_j} = \tilde{\boldsymbol{c}}_j$, and $\widehat{\otimes^2 \tilde{\boldsymbol{c}}_j} = \tilde{\boldsymbol{c}}_j \otimes \tilde{\boldsymbol{c}}_j - \frac{1}{3}|\tilde{\boldsymbol{c}}_j|^2 \mathbb{I}$. Here both $\Psi^{\mathcal{D}_i}$ and $\eta^{\mathcal{D}_i}$ are written with respect to this basis. That is, $\Psi^{\mathcal{D}_i}$ is fully determined as a linear function of the first basis function ϕ_{1000j}, while $\eta^{\mathcal{D}_i}$ is weighted by the coefficient matrix $\beta^{\mathcal{D}_i}$ such that $\eta^{\mathcal{D}_i} = \sum_{sj} \beta^{\mathcal{D}_i}_{sj} \phi_{sj}$, where s denotes the set of function type indices corresponding to the basis, and j is the species index.

Then due to the orthogonality condition on the product on the right side of (2.27), recasting (2.27) in the basis $\left(\mathfrak{F}(\eta^{\mathcal{D}_i}), \phi\right)_{mcs} = \left(\Psi^{\mathcal{D}_i}, \phi\right)_{mcs}$ gives us the form: $\mathscr{L}\boldsymbol{\beta}^{\mathcal{D}_i} = \boldsymbol{\gamma}^{\mathcal{D}_i}$, where $\boldsymbol{\gamma}^{\mathcal{D}_i}$ corresponds to the coefficients of $\Psi^{\mathcal{D}_i}$ in the basis. Here $\mathscr{L}$ is an appropriately scaled type of mass matrix in the symmetric bilinear positive semi-definite form $[\phi_{a0cdj}, \phi_{a0cdj}]$. By using this matrix representation $\mathscr{L}\boldsymbol{\beta}^{\mathcal{D}_i} = \boldsymbol{\gamma}^{\mathcal{D}_i}$ we recover the $\boldsymbol{\beta}^{\mathcal{D}_i}$.

Returning to the variational form (2.27) we then notice that,

$$[\eta^{\mathcal{D}_i}, \eta^{\mathcal{D}_j}] = \left(\Psi^{\mathcal{D}_i}, \eta^{\mathcal{D}_j}\right)_{mcs}, \text{ yielding } \left(\Psi^{\mathcal{D}_i}, \eta^{\mathcal{D}_j}\right)_{mcs} = \sum_{sk} \beta^{\mathcal{D}_i}_{sk} \gamma^{\mathcal{D}_j}_{rk}. \tag{2.28}$$

Finally we employ the constraint equation from (2.26), where

$$\left(\mathcal{T}\hat{\psi}_\ell, \eta^{\mathcal{D}_j}\right)_{mcs} = 0, \text{ explicitly provides the constraint } \sum_k \alpha_k \beta^{\mathcal{D}_j}_{1000k} = 0,$$

where again the orthogonality of the basis yields the right side. This is enough then to fully recover the diffusion matrix $\mathcal{D}_{ij}$ from (2.24) since the Enskog expansion in η_i provides that:

$$\mathcal{D}_{ij} = \frac{p k_b \vartheta}{3} [\eta^{\mathcal{D}_i}, \eta^{\mathcal{D}_j}].$$

Let us recall two salient features of the mass diffusion coefficient $\mathscr{D}_i$ in (2.24) as dictated by the physical derivation: first, the species weighted diffusion matrix $\mathrm{diag}(\rho_i)\mathcal{D}$ with diagonal components $\rho_i \mathcal{D}_{ij}$ are C^∞ functions of $\boldsymbol{\alpha} = (\alpha_1, \ldots, \alpha_n)$ and ϑ, where $\vartheta > 0$ and $\boldsymbol{\alpha} \geq 0$, $\boldsymbol{\alpha} \neq 0$; second, the matrix $\mathrm{diag}(\rho_i)\mathcal{D}$ with diagonal components $\rho_i \mathcal{D}_{ij}$ is a symmetric positive semidefinite matrix, and satisfies the ellipticity condition in the inner product, $(\mathrm{diag}(\rho_i)\mathcal{D}\boldsymbol{\zeta}, \boldsymbol{\zeta}) \geq \varpi(\vartheta) z (\mathrm{diag}(\alpha_i)\boldsymbol{\zeta}, \boldsymbol{\zeta})$ for a constant $z > 0$ and any $\boldsymbol{\zeta} \in \mathbb{R}^n$ and $\boldsymbol{x} \in \Omega$, given a function $\varpi(\vartheta) > 0$. Thus by virtue of the state equation in p (the ideal gas law) we recover the necessary bounds on $\mathscr{D}_i$ required in [44], which is namely that $\mathscr{D}_i \in (L^\infty(\Omega))^{N \times N}$ and that due to the bound on the thermal variation, there exists a positive constant $\mathfrak{z}$ such that $\mathscr{D}_i(\boldsymbol{x})\boldsymbol{\xi} \cdot \boldsymbol{\xi} \geq \mathfrak{z}|\boldsymbol{\xi}|^2$ for $\boldsymbol{\xi} \in \mathbb{R}^N$ and $\boldsymbol{x} \in \Omega$.

Finally, let us just recall the case of chemical equilibrium as discussed in §2.1. As discussed, we can treat this case as simply satisfying the same equation arising in the strong and Maxwellian reaction regimes, except for that the transport coefficients satisfy a different form. The full derivation of the form these coefficients take can be found in [36]. Likewise we can introduce the "exact regimes" discussed in §2.1, where the diffusion is derived from the species Boltzmann equation directly. Numerically this is accomplished by introducing an interchange function $\mathscr{I}_i$, which in the quiescent reactor regime is given by

$$\mathscr{I}_i = \begin{cases} \tilde{\mathscr{D}}_i, & \text{if } \mathscr{A}_i(\mathring{n}) < \varepsilon \quad \forall i \\ \mathscr{D}_i, & \text{otherwise} \end{cases}$$

where $\tilde{\mathscr{D}}_i$ is the diffusion coefficient derived in the case of $b = -1$, and ε is a numerical tolerance. For the exact case we simply set $\mathscr{D}_i$ to be the precise form of the mass diffusivity coefficient, instead of its variational counterpart.

Hence, letting $\mathscr{I} = (\mathscr{I}_1, \ldots, \mathscr{I}_n)^\top$ and using the same split notation as above, we account for this behavior by rewriting (2.20) in the form:

$$\text{fast/slow diffusion modes} \begin{cases} (\boldsymbol{\rho}_f)_t - \nabla_x \cdot (\mathscr{I}_f \boldsymbol{\sigma}_f) = 0, & \text{with} \quad \boldsymbol{\sigma}_f - \nabla_x \boldsymbol{\rho}_f = 0, \\ (\boldsymbol{\rho}_s)_t - \nabla_x \cdot (\mathscr{I}_s \boldsymbol{\sigma}_s) = 0, & \text{with} \quad \boldsymbol{\sigma}_s - \nabla_x \boldsymbol{\rho}_s = 0, \end{cases} \tag{2.29}$$

which will be the split diffusion equation we are interested in solving approximately below.

§2.6 **Spatial discretization**

Let us now characterize the spatial discretization used for the numerical solution methods. Take an open $\Omega \subset \mathbb{R}$ with boundary $\partial\Omega = \Gamma$, given $T > 0$ such that $\mathcal{Q}_T = ((0, T) \times \Omega)$. Let $\mathscr{T}_h$ denote the partition of the closure

of the polygonal triangulation of Ω, which we denote Ω_h, into a finite number of polygonal elements denoted Ω_e, such that $\mathscr{T}_h = \{\Omega_{e_1}, \Omega_{e_2}, \ldots, \Omega_{e_{ne}}\}$, for $ne \in \mathbb{N}$ the number of elements in Ω_h. In what follows, we define the mesh diameter h to satisfy $h = \min_{ij}(d_{ij})$ for the distance function $d_{ij} = d(\boldsymbol{x}_i, \boldsymbol{x}_j)$ and elementwise face vertices $\boldsymbol{x}_i, \boldsymbol{x}_j \in \partial\Omega_e$ when the mesh is structured and regular. For unstructured meshes we mean the average value of h over the mesh unless we are in the h-adaptive regime, in which case the mesh is structured.

Now, let Γ_{ij} denote the face shared by two neighboring elements Ω_{e_i} and Ω_{e_j}, and for $i \in I \subset \mathbb{Z}^+ = \{1, 2, \ldots\}$ define the indexing set $r(i) = \{j \in I : \Omega_{e_j} \text{ is a neighbor of } \Omega_{e_i}\}$. Let us denote all boundary faces of Ω_{e_i} contained in $\partial\Omega_h$ by S_j and letting $I_B \subset \mathbb{Z}^- = \{-1, -2, \ldots\}$ define $s(i) = \{j \in I_B : S_j \text{ is a face of } \Omega_{e_i}\}$ such that $\Gamma_{ij} = S_j$ for $\Omega_{e_i} \in \Omega_h$ when $S_j \in \partial\Omega_{e_i}$, $j \in I_B$. Then for $\Xi_i = r(i) \cup s(i)$, we have

$$\partial\Omega_{e_i} = \bigcup_{j \in \Xi(i)} \Gamma_{ij}, \quad \text{and} \quad \partial\Omega_{e_i} \cap \partial\Omega_h = \bigcup_{j \in s(i)} \Gamma_{ij}.$$

We are interested in obtaining an approximate solution to $\boldsymbol{U}$ at time t on the finite dimensional space of discontinuous piecewise polynomial functions over Ω restricted to $\mathscr{T}_h$, given as

$$S_h^p(\Omega_h, \mathscr{T}_h) = \{\boldsymbol{v} : v_{|\Omega_{e_i}} \in \mathscr{P}^p(\Omega_{e_i}), \ \ \forall v \in \boldsymbol{v}, \ \ \forall \Omega_{e_i} \in \mathscr{T}_h\}$$

for $\mathscr{P}^p(\Omega_{e_i})$ the space of degree $\leq p$ polynomials over Ω_{e_i}.

Choosing a set of degree p polynomial basis functions $N_l \in \mathscr{P}^p(\mathcal{G}_i)$ for $l = 0, \ldots, n_p$ the corresponding degrees of freedom, we can denote the state vector at time t over Ω_h, by

$$\boldsymbol{\rho}_{hp}(t, \boldsymbol{x}) = \sum_{l=0}^{n_p} \boldsymbol{\rho}_l^i(t) N_l^i(\boldsymbol{x}), \quad \forall \boldsymbol{x} \in \Omega_{e_i},$$

where the N_l^i's are the finite element shape functions in the DG setting, and the $\boldsymbol{\rho}_l^i$'s correspond to the nodal coordinates. The finite dimensional test functions $\boldsymbol{\varphi}_{hp}, \boldsymbol{\varsigma}_{hp}, \boldsymbol{\varpi}_{hp} \in W^{k,q}(\Omega_h, \mathscr{T}_h)$ are characterized by

$$\boldsymbol{\varphi}_{hp}(\boldsymbol{x}) = \sum_{l=0}^{p} \boldsymbol{\varphi}_l^i N_l^i(\boldsymbol{x}), \quad \boldsymbol{\varsigma}_{hp}(\boldsymbol{x}) = \sum_{l=0}^{p} \boldsymbol{\varsigma}_l^i N_l^i(\boldsymbol{x}) \quad \text{and} \quad \boldsymbol{\varpi}_{hp}(\boldsymbol{x}) = \sum_{l=0}^{p} \boldsymbol{\varpi}_l^i N_l^i(\boldsymbol{x}) \quad \forall \boldsymbol{x} \in \Omega_{e_i},$$

where $\boldsymbol{\varphi}_\ell^i$, $\boldsymbol{\varsigma}_\ell^i$ and $\boldsymbol{\varpi}_\ell^i$ are the nodal values of the test functions in each Ω_{e_i}, and with the broken Sobolev space over the partition $\mathscr{T}_h$ defined by

$$W^{k,q}(\Omega_h, \mathscr{T}_h) = \{\boldsymbol{w} : w_{|\Omega_{e_i}} \in W^{k,q}(\Omega_{e_i}), \ \ \forall w \in \boldsymbol{w}, \ \forall \Omega_{e_i} \in \mathscr{T}_h\}.$$

Now, by virtue of §2.2 we split the reaction and the diffusion parts of (2.18) into separate equations (where each part may contain its requisite "fast" and "slow" parts). We thus multiply (2.29), (2.19), and the auxiliary equations by the test functions $\boldsymbol{\varsigma}_{hp}$, $\boldsymbol{\varpi}_{hp}$ and $\boldsymbol{\varphi}_{hp}$ and then integrate locally over elements Ω_{e_i} in space. Defining the global scalar product by $(\boldsymbol{a}_{hp}, \boldsymbol{b}_{hp})_{\Omega_\mathcal{G}} = \sum_{\Omega_{e_i} \in \mathscr{T}_h} \int_{\Omega_{e_i}} \boldsymbol{a}_{hp} \odot \boldsymbol{b}_{hp} dx$, we then obtain:

$$\begin{aligned} \frac{d}{dt}\left(\boldsymbol{\rho}, \boldsymbol{\varsigma}_{hp}\right)_{\Omega_\mathcal{G}} &= \left(\nabla_x \cdot (\mathscr{J}\boldsymbol{\sigma}), \boldsymbol{\varsigma}_{hp}\right)_{\Omega_\mathcal{G}}, \quad \left(\boldsymbol{\sigma}, \boldsymbol{\varpi}_h\right)_{\Omega_\mathcal{G}} - \left(\nabla_x \boldsymbol{\rho}, \boldsymbol{\varpi}_h\right)_{\Omega_\mathcal{G}} = 0, \\ \frac{d}{dt}\left(\boldsymbol{\rho}, \boldsymbol{\varphi}_{hp}\right)_{\Omega_\mathcal{G}} &= \left(\mathscr{A}(\mathring{\boldsymbol{n}}), \boldsymbol{\varphi}_{hp}\right)_{\Omega_\mathcal{G}}. \end{aligned} \tag{2.30}$$

We proceed by approximating each term of (2.30) in the usual DG sense, which yields for the temporal derivative terms that

$$\frac{d}{dt}\left(\boldsymbol{\rho}_{hp}, \boldsymbol{\varsigma}_{hp}\right)_{\Omega_\mathcal{G}} \approx \frac{d}{dt}\left(\boldsymbol{\rho}, \boldsymbol{\varsigma}_{hp}\right)_{\Omega_\mathcal{G}} \quad \text{and} \quad \frac{d}{dt}\left(\boldsymbol{\rho}_{hp}, \boldsymbol{\varphi}_{hp}\right)_{\Omega_\mathcal{G}} \approx \frac{d}{dt}\left(\boldsymbol{\rho}, \boldsymbol{\varphi}_{hp}\right)_{\Omega_\mathcal{G}}, \tag{2.31}$$

and likewise for the mass action term that,

$$\left(\mathscr{A}_{hp}(\mathring{\boldsymbol{n}}), \boldsymbol{\varphi}_{hp}\right)_{\Omega_\mathcal{G}} \approx \left(\mathscr{A}(\mathring{\boldsymbol{n}}), \boldsymbol{\varphi}_{hp}\right)_{\Omega_\mathcal{G}}. \tag{2.32}$$

Now, let $\boldsymbol{n}_{ij}$ be the unit outward normal to $\partial\Omega_{e_i}$ on Γ_{ij}, and let $\varphi_{|\Gamma_{ij}}$ and $\varphi_{|\Gamma_{ji}}$ denote the values of φ on Γ_{ij} considered from the interior and the exterior of Ω_{e_i}, respectively. Then the mass diffusion term from (2.30), after an integration by parts, yields,

$$(\nabla_x \cdot (\mathscr{I}\boldsymbol{\sigma}), \varsigma_{hp})_{\Omega_{\mathcal{G}}} = \sum_{\Omega_{e_i}\in\mathscr{T}_h} \int_{\Omega_{e_i}} \nabla_x \cdot (\varsigma_{hp}\mathscr{I}\boldsymbol{\sigma})dx - (\mathscr{I}\boldsymbol{\sigma}, \nabla_x\varsigma_{hp})_{\Omega_{\mathcal{G}}}\,, \tag{2.33}$$

such that we approximate the first term on the right in (2.33) using the generalized flux $\mathring{\mathscr{G}}_{ij}$ in the unified setting (see [2, 3]) across the boundary, such that $\mathscr{G}_i = \mathscr{G}_i(\mathscr{I}_{hp}, \boldsymbol{\sigma}_{hp}, \boldsymbol{\rho}_{hp}, \varsigma_{hp})$, and we see that

$$\begin{aligned}\mathscr{G}_i &= \sum_{j\in S(i)} \int_{\Gamma_{ij}} \mathring{\mathscr{G}}_{ij}(\mathscr{I}_{hp}, \boldsymbol{\sigma}_{hp}|_{\Gamma_{ij}}, \boldsymbol{\sigma}_{hp}|_{\Gamma_{ji}}, \boldsymbol{\rho}_{hp}|_{\Gamma_{ij}}, \boldsymbol{\rho}_{hp}|_{\Gamma_{ji}}, \boldsymbol{n}_{ij}) \cdot \varsigma_{hp}|_{\Gamma_{ij}} d\Xi \\ &\approx \sum_{j\in S(i)} \int_{\Gamma_{ij}} \sum_{s=1}^{N} (\mathscr{I}_{hp}\boldsymbol{\sigma})_s \cdot (n_{ij})_s \varsigma_{hp}|_{\Gamma_{ij}} d\Xi.\end{aligned} \tag{2.34}$$

It is important to note here that $\mathscr{I}_{hp} = \mathscr{I}|_{\Omega_{e_i}}$ is the mass diffusion interchange evaluated locally on the corresponding element interior, which agrees on every face of the base elements boundary, but is determined by the flux formulation across neighboring elements (for example, averaged etc.). The interior term in (2.33) is approximated directly by:

$$\mathscr{H} = \mathscr{H}(\mathscr{I}_{hp}, \boldsymbol{\sigma}_h, \boldsymbol{\rho}_{hp}, \varsigma_{hp}) = \left(\mathscr{I}_{hp}\boldsymbol{\sigma}_{hp}, \varsigma_x^{hp}\right)_{\Omega_{\mathcal{G}}} \approx \left(\mathscr{I}\nabla_x\boldsymbol{\rho}, \varsigma_x^{hp}\right)_{\Omega_{\mathcal{G}}}. \tag{2.35}$$

Finally, for the auxiliary equation in (2.30), a numerical flux is also chosen, satisfying:

$$\begin{aligned}\mathscr{L}_i = \mathscr{L}_i(\mathring{\mathscr{L}}_{ij}, \boldsymbol{\sigma}_{hp}, \boldsymbol{\rho}_{hp}, \boldsymbol{\varpi}_{hp}, \boldsymbol{\varpi}_x^{hp}, \boldsymbol{n}_{ij}) &= (\boldsymbol{\sigma}_{hp}, \boldsymbol{\varpi}_{hp})_{\Omega_{e_i}} + \left(\boldsymbol{\rho}_{hp}, \boldsymbol{\varpi}_x^{hp}\right)_{\Omega_{e_i}} \\ &\quad - \sum_{j\in S(i)} \int_{\Gamma_{ij}} \mathring{\mathscr{L}}(\boldsymbol{\rho}_{hp}|_{\Gamma_{ij}}, \boldsymbol{\rho}_{hp}|_{\Gamma_{ji}}, \boldsymbol{\varpi}_{hp}|_{\Gamma_{ij}}, \boldsymbol{n}_{ij})d\Xi,\end{aligned} \tag{2.36}$$

$$\text{where} \quad \sum_{j\in S(i)} \int_{\Gamma_{ij}} \mathring{\mathscr{L}}_{ij}(\boldsymbol{\rho}_{hp}|_{\Gamma_{ij}}, \boldsymbol{\rho}_{hp}|_{\Gamma_{ji}}, \boldsymbol{\varpi}_{hp}|_{\Gamma_{ij}}, \boldsymbol{n}_{ij})d\Xi \approx \sum_{j\in S(i)} \int_{\Gamma_{ij}} \sum_{s=1}^{N} (\boldsymbol{\rho})_s \cdot (n_{ij})_s \boldsymbol{\varpi}_{hp}|_{\Gamma_{ij}} d\Xi.$$

§2.7 **Formulation of the problem**

Combining (2.31), (2.32) and (2.34)–(2.36) while setting $\mathscr{X} = \sum_{\mathcal{G}_i\in\mathscr{T}_h} \mathscr{X}_i$, we can then formulate the semidiscrete approximate solution to (2.11) as the problem: for each $t > 0$, find the pair $(\boldsymbol{\rho}_{hp}, \boldsymbol{\sigma}_{hp})$ such that

The semidiscrete discontinuous Galerkin scheme

$$\begin{aligned}&a) \quad \boldsymbol{\rho}_{hp} \in C^1([0,T); S_h^d),\ \boldsymbol{\sigma}_{hp} \in S_h^d, \\ &b) \quad \boldsymbol{\rho}_{hp}(0) = \Pi_{hp}\boldsymbol{\rho}_0, \\ &c) \quad \frac{d}{dt}\left(\boldsymbol{\rho}_{hp}, \varsigma_{hp}\right)_{\Omega_{\mathcal{G}}} = \mathscr{G} + \mathscr{H}, \quad \mathscr{L} = 0, \\ &d) \quad \frac{d}{dt}\left(\boldsymbol{\rho}_{hp}, \boldsymbol{\varphi}_{hp}\right)_{\Omega_{\mathcal{G}}} = \left(\mathscr{A}_{hp}(\mathring{\boldsymbol{n}}), \boldsymbol{\varphi}_{hp}\right)_{\Omega_{\mathcal{G}}}.\end{aligned} \tag{2.37}$$

Note that the boundary forcings are implicit here, where every element is summed over, including every boundary face. Also, by Π_{hp} we denote the projection operator onto the space of discontinuous piecewise polynomials S_h^p, and where below we always utilize a standard L^2–projection on the initial conditions. In other words, given a function $\boldsymbol{f}_0 \in L^2(\Omega_{e_i})$, the approximate local projection $\boldsymbol{f}_{0,h} \in L^2(\Omega_{e_i})$ is obtained by solving, $\int_{\Omega_{e_i}} \boldsymbol{f}_{0,h}\boldsymbol{v}_h dx = \int_{\Omega_{e_i}} \boldsymbol{f}_0\boldsymbol{v}_h dx$.

§2.7.1 **The time discretization**

In order to discretize the time derivatives in (2.37*c*-*d*) we employ a family of Runge-Kutta schemes as discussed in [43, 73, 75]. That is, we rewrite (2.37*c*-*d*) in the form: $\boldsymbol{M}\boldsymbol{\rho}_t = \mathcal{L}$, where $\mathcal{L} = \mathcal{L}(\boldsymbol{\rho}, \boldsymbol{\sigma})$ is the reaction–diffusion contribution, and where $\boldsymbol{M}$ is the corresponding mass matrix. Then the generalized χ stage of order $\mathfrak{T}$ Runge-Kutta method (denoted RK$(\chi, \mathfrak{T})$) may be written to satisfy:

$$\begin{aligned}
&\boldsymbol{\rho}^{(0)} = \boldsymbol{\rho}^n,\\
&\boldsymbol{\rho}^{(i)} = \sum_{r=0}^{i-1}\left(\breve{\lambda}_{ir}\boldsymbol{\rho}^r + \Delta t^n \tilde{\lambda}_{ir}\boldsymbol{M}^{-1}\mathcal{L}^r\right), \quad \text{for } \; i = 1, \ldots, \chi\\
&\boldsymbol{\rho}^{n+1} = \boldsymbol{\rho}^{(\chi)},
\end{aligned} \tag{2.38}$$

where $\mathcal{L}^r = \mathcal{L}(\boldsymbol{\rho}^r, \boldsymbol{\sigma}^r, \boldsymbol{x}, t^n + \delta_r \Delta t^n)$, and the solution at the n–th timestep is given as $\boldsymbol{U}^n = \boldsymbol{U}_{|t=t^n}$ and at the n–th plus first timestep by $\boldsymbol{U}^{n+1} = \boldsymbol{U}_{|t=t^{n+1}}$, with $t^{n+1} = t^n + \Delta t^n$. The $\breve{\lambda}_{ir}$ and $\tilde{\lambda}_{ir}$ are the coefficients arising from the Butcher Tableau, and the fourth argument in $\mathcal{L}^r$ corresponds to the time-lag constraint where $\delta_r = \sum_{l=0}^{r-1}\mu_{rl}$ given $\mu_{ir} = \tilde{\lambda}_{ir} + \sum_{l=r+1}^{i-1}\mu_{lr}\breve{\lambda}_{il}$ for $\breve{\lambda}_{ir} \geq 0$ satisfying $\sum_{r=0}^{i-1}\breve{\lambda}_{ir} = 1$.

Then we recast (2.37) in the fully discrete setting as follows. For each fast step $\Delta t^{n_f} = \Delta t^{n_s}/2m$ where $m \in \mathbb{N}$ and n_s corresponds to the slow step, such that $n_f, n_s > 0$ as arising in $t^{n_s} \geq t^{n_f} > t^0$ (see Figure 2), find the slow pair $(\boldsymbol{\rho}_{hp}^{n_s}, \boldsymbol{\sigma}_{hp}^{n_s})$ (that is, the fast/slow mode pair) such that:

The discrete split explicit RK discontinuous Galerkin scheme

$$\begin{aligned}
&a) \quad \boldsymbol{\rho}_{hp}(0) = \Pi_{hp}\boldsymbol{\rho}_0,\\
&b) \quad \boldsymbol{\rho}_{hp}^{n_f} = \boldsymbol{\rho}_{hp}(0),\\
&cd) \quad \left(\boldsymbol{\rho}_{hp}^{n_s+1}, \boldsymbol{\varsigma}_{hp}\right)_{\Omega_{\mathcal{G}}} = \left(\boldsymbol{\rho}_{hp}^{(\chi)}, \boldsymbol{\varsigma}_{hp}\right)_{\Omega_{\mathcal{G}}}, \quad \mathscr{L}^{(\chi-1)} = 0,\\
&dc) \quad \left(\boldsymbol{\rho}_{hp}^{n_s+1}, \boldsymbol{\varphi}_{hp}\right)_{\Omega_{\mathcal{G}}} = \left(\boldsymbol{\rho}_{hp}^{(\chi)}, \boldsymbol{\varphi}_{hp}\right)_{\Omega_{\mathcal{G}}}.\\
&e) \quad \mathfrak{Y}^{\mathfrak{T}} = \mathfrak{Y}^{\mathfrak{T}}(\mathcal{D}, \mathcal{R}, t^{n_s+1}).
\end{aligned} \tag{2.39}$$

Here for every slow step n_s, $2m$ fast steps n_f must be solved in order to appropriately evaluate e (which requires the mn_f step), where the form that $\mathfrak{Y}^{\mathfrak{T}}$ takes depends first on whether the reaction step dc or the diffusion step cd is fast/slow, and second what order accurate scheme one imposes on the solution. Clearly the RK step (2.38) and the asymptotic accuracy of the splitting method (2.39e) must correspond in order to achieve a fixed top order accurate method in time. Also note that the evaluation method also depends on the strategy employed in the mass action. When the fully coupled strategy is utilized, for example, step d from (2.37) merely becomes an L^2-projection of the exact time-dependent solution at timestep t^{n_s} or t^{n_f}, and no temporal quadrature is necessary, while in the case of the approximate strategy, the integrator must be employed.

In the remainder of this particular paper, we will be interested in time order accuracy less than third order. This helps to explain the choice of an SSPRK scheme, which is really a methodology developed for stability methods in advective transport problems. In this sense we view (2.39) as a pre-convective strategy, in the sense that it is well-suited for an extension to a full convective–reaction–diffusion problem. However, in our reaction–diffusion regime, its justification comes from the fact that up to third order an equivalency exists between RKSSP methods and explicit Runge-Kutta-Chebyshev (RKC) methods with infinite damping parameter ($\epsilon \to \infty$) designed for handling arbitrary parabolic PDEs. Up to this restriction we expect good stability for quiescent reaction chemistry with relatively mild (non-stiff) oscillations (up to the time–stepping factor m). The drawback of the RKSSP schemes is that infinite damping leads to a substantial contracting of the corresponding stability region (e.g. see [86]).

To recover the more optimal thin region stability (see [83, 85]) we alternatively adopt the finite damped

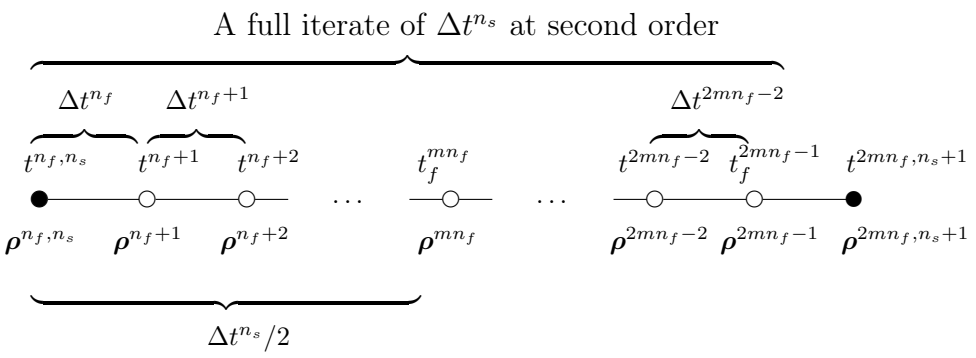

Figure 2: Here we show the time integration with respect to the splitting method from §2.2 in the fully discrete setting, corresponding to step e in (2.39) for the second order accurate Strang splitting from §2.3.

RKC method of second order, where (2.38) is replaced by

$$\begin{aligned}
\boldsymbol{\rho}^{(0)} &= \boldsymbol{\rho}^n, \\
\boldsymbol{\rho}^{(1)} &= \boldsymbol{\rho}^{(0)} + \Delta t^n \tilde{\mu}_1 \boldsymbol{M}^{-1} \mathcal{L}^0 \\
\boldsymbol{\rho}^{(j)} &= (1 - \hat{\mu}_j - \hat{\nu}_j)\, \boldsymbol{\rho}^{(0)} + \hat{\mu}_j \boldsymbol{\rho}^{(j-1)} + \hat{\nu}_j \boldsymbol{\rho}^{(j-2)} \\
&\qquad + \Delta t^n \tilde{\mu}_j \boldsymbol{M}^{-1} \mathcal{L}^{j-1} + \Delta t^n \tilde{\gamma}_j \boldsymbol{M}^{-1} \mathcal{L}^0 \quad \text{for } j \in \{2, \dots, \chi\} \\
\boldsymbol{\rho}^{n+1} &= \boldsymbol{\rho}^{(\chi)}.
\end{aligned} \tag{2.40}$$

Here, $\tilde{\mu}_1 = \omega_1 \omega_0^{-1}$ and for each $j \in \{2, \dots, \chi\}$:

$$\begin{gathered}
\hat{\mu}_j = \frac{2\hat{b}_j \omega_0}{\hat{b}_{j-1}}, \quad \hat{\nu}_j = \frac{-\hat{b}_j}{\hat{b}_{j-2}}, \quad \tilde{\mu}_j = \frac{2\hat{b}_j \omega_1}{\hat{b}_{j-1}} \quad \tilde{\gamma}_j = a_{j-1}\tilde{\mu}_j, \\
\text{where} \quad a_j = 1 - b_j T_j(\omega_0), \quad \hat{b}_0 = \hat{b}_2, \quad \hat{b}_1 = \omega_0^{-1} \quad \hat{b}_j = T_j''(\omega_0) T_j'(\omega_0)^{-2}, \quad \text{for} \quad j \in \{2, \dots, \chi\}, \\
\text{with } \omega_0 = 1 + \epsilon \chi^{-2}, \quad \omega_1 = T_\chi'(\omega_0) T_\chi''(\omega_0)^{-1},
\end{gathered}$$

where the T_j are the Chebyshev polynomials of the first kind, and U_j the Chebyshev polynomials of the second kind which define the derivatives, given by the recursion relations:

$$\begin{aligned}
&T_0(x) = 1, \quad T_1(x) = x, \qquad T_j(x) = 2xT_{j-1}(x) - T_{j-2}(x) \quad \text{for} \quad j \in \{2, \dots, \chi\}, \\
&U_0(x) = 1, \quad U_1(x) = 2x, \quad U_j(x) = 2xU_{j-1}(x) - U_{j-2}(x) \quad \text{for} \quad j \in \{2, \dots, \chi\}, \\
&T_j'(x) = jU_{j-1}, \quad T_j''(x) = \left(j \frac{(n+1)T_j - U_j}{x^2 - 1} \right) \quad \text{for} \quad j \in \{2, \dots, \chi\}.
\end{aligned}$$

Finally the operator $\mathcal{L}^j$ is evaluated at time $\mathcal{L}^j(t^n + \tilde{c}_j \Delta t^n)$, where the $\tilde{c}_j$ are given by:

$$c_0 = 0, \quad c_1 = \tfrac{1}{4} c_2 \omega_0^{-1}, \quad c_j = \frac{T_\chi'(\omega_0) T_j''(\omega_0)}{T_\chi''(\omega_0) T_j'(\omega_0)} \approx \frac{j^2 - 1}{\chi^2 - 1} \quad \text{for } j \in \{2, \dots, \chi - 1\}, \quad c_\chi = 1.$$

Notice that in contrast to the SSPRK schemes where the stage expansion is used to thicken the stability region along the admissible imaginary axis while reducing the number of stable negative real eigenvalues along the real axis, in the RKC methods the stage expansion is used to lengthen the stability region along the real axis, as discussed at length in [83].

Such temporal discretizations can always be performed, but in the explicit methodology the timestep restriction often becomes too severe to efficiently model realistic systems. To recover these restrictive stiff reactions, we implement an implicit/explicit (IMEX) splitting strategy along the reaction modes of the system and maintain either the SSPRK or the RKC strategy in the more easily stabilized diffusion modes.

The discrete split IMEX discontinuous Galerkin scheme

$$
\begin{aligned}
&a) \quad \boldsymbol{\rho}_{hp}(0) = \Pi_{hp}\boldsymbol{\rho}_0,\\
&b) \quad \boldsymbol{\rho}_{hp}^{n_f} = \boldsymbol{\rho}_{hp}(0),\\
&cd) \quad \left(\boldsymbol{\rho}_{hp}^{n_s+1}, \boldsymbol{\varsigma}_{hp}\right)_{\Omega_{\mathcal{G}}} = \left(\boldsymbol{\rho}_{hp}^{(\chi)}, \boldsymbol{\varsigma}_{hp}\right)_{\Omega_{\mathcal{G}}}, \quad \mathscr{L}^{(\chi-1)} = 0,\\
&dc) \quad \left(\boldsymbol{\rho}_{hp}^{n_s+1}, \boldsymbol{\varphi}_{hp}\right)_{\Omega_{\mathcal{G}}} = \left(\boldsymbol{\rho}_{hp}^{n_s}, \boldsymbol{\varphi}_{hp}\right)_{\Omega_{\mathcal{G}}} + \Delta t^{n_s}\mathscr{Z}\left(\mathscr{A}_{hp}(\mathring{\boldsymbol{n}}), \boldsymbol{\varphi}_{hp}\right).\\
&e) \quad \mathfrak{Y}^{\mathfrak{T}} = \mathfrak{Y}^{\mathfrak{T}}(\mathcal{D}, \mathcal{R}, t^{n_s+1}).
\end{aligned}
\tag{2.41}
$$

Here the implicit timestepping in (2.41-dc) is chosen such that we implement the usual back differentiation formulas (BDF(k)) of order k. Hence at first and second order, the $\mathscr{Z} = \mathscr{Z}(\mathscr{A}_{hp}(\mathring{\boldsymbol{n}}), \boldsymbol{\varphi}_{hp})$ in (2.41-dc) become the backward Euler and Crank-Nicolson methods, respectively. In either case (2.41) is set using Newton–Krylov methods with low accuracy tolerances (as in [71]) such that the explicit diffusion step stability is taken as the stability limiting step. By default the Krylov method used is GMRES, while the Newton iteration is based on standard Jacobian line search methods, where background discussions can be found in [16, 24, 55].

Note that in [71] recent numerical stability analysis has been done on a closely related reaction-diffusion scheme, which amounts to (2.41) where the explicit diffusion step is replaced with an implicit scheme, in particular, in the first order with backward Euler and in the second order with the implicit trapezoidal rule. Since we are contextualized in the setting of DG methods, and since we are interested in "pre-convective" schemes, it is of interest to know how well the IMEX splitting performs relative to these fully implicit methods, where the timestep restriction in its most admissible formulation is restricted by the C-stability bounds (see [71] for the theorem).

Such operator splitting schemes have been recently studied in [29, 30] for reaction-diffusion problems. For example, in [30] the fully implicit scheme is shown to lead to a well-posed system of reaction-diffusion equations, providing the existence of an entropic structure and a partial equilibrium manifold. In this context some important results are obtained on controlling the splitting error of the method (as previously mentioned in §2.3). Nevertheless, the partial equilibrium structure discussed in [30, 41] is quite a strong assumption leading to highly "relaxed" dynamical systems. These assumptions seem necessary in order to recovered well-posedness features of a C^∞ solution, since the associated nFANODE arising from the mass action in §2.4 display rudimentary discontinuities even in (relatively) simple systems. Moreover the prevalence of traveling wave front solutions indicate further singular behavior [69]. In fact, recent work has shown that even for weak solutions with at most a quadratic mass action [13, 44], when $N > 2$ singular neighborhoods are not only expected, but as shown in [44], the Hausdorff dimension of the singularity set $\mathfrak{V}$ of the global solution has computable upper bound, $\dim_{\mathcal{H}}\mathfrak{V} \leq N^2 - 4/N$.

Thus, in order to further stabilize our (non-filtered) variational solutions we utilize an exact entropic restriction as outlined in §3 below, based on the regularity results of A. Vasseur, T. Goudon and C. Caputo [18, 44], which depends strongly on an explicit analytic entropy functional $\mathscr{S}_{\mathfrak{R}}$. These results extend the sensitivity analysis around the equilibrium solutions of [30, 41] to include global L^∞ solutions for $N \leq 2$. As noted above, when $N > 2$, no such global regularity is expected, and as a result, it is important to develop numerical methods that can filter out these singular sets.

As a step in this direction, we enforce numerical entropy consistency on our solution by way of an *a posteriori* calculation, which provides a variational bound on the systems entropy, but we further expand this entropic structure to serve as the foundation for a dynamic *hp*-adaptive strategy as derived in detail in §3. The basic idea, as we will discuss in some detail, is to refine/coarsen and enrich/de-enrich in areas displaying either "singular behavior" or "excessive regularity" in order to average out the local behavior over the integral element.

§3 Entropy enriched *hp*-adaptivity and stability

§3.1 Bounded entropy in quiescent reactors

Let us derive the entropy of the system $\mathscr{S}_{\mathfrak{R}}$ over each reaction $r \in \mathfrak{R}$ in the quiescent regime. First notice that $m_i\partial_t n_i = m_i n_i \partial_t(\ln n_i)$. Now we will make use of the following positive species-dependent constant $\mathring{\kappa}_i$, which

is written in terms of each reactions equilibrium constant $K_{eq,r} = k_{fr}k_{br}^{-1}$ such that,

$$\mathring{\kappa}_i = \left[\prod_{r\in\mathfrak{R}} K_{eq,r}\right]^{-1/n(\sum_{r\in\mathfrak{R}}(\nu_{ir}^b-\nu_{ir}^f))}.$$

Now multiplying (2.11) by $\mathring{\kappa}_i$ and then another copy of (2.11) by $\ln(\mathring{\kappa}_i n_i)$, dividing by a constant, summing the equations together and integrating by parts we obtain the relation:

$$\frac{d}{dt}\sum_{i=0}^{n}\int_\Omega n_i\left(\ln(\mathring{\kappa}_i n_i)+\mathring{\kappa}_i\right)dx - \int_\Omega\sum_{i=0}^{n}\ln\left(n_i\mathring{\kappa}_i\right)\nabla_x\cdot(\mathscr{D}_i\nabla_x n_i)dx = \int_\Omega\sum_{i=0}^{n} m_i^{-1}\mathscr{A}_i(\mathring{n})\odot_{r\in\mathfrak{R}}\ln\left(n_i\mathring{\kappa}_i\right)dx,$$

where it is important to recall the conservation principle from (2.16). The product $\odot_{r\in\mathfrak{R}}$ is simply the standard scalar product with respect to the r of $\mathfrak{R}$, such that for any two functions w_r and y_r the term $\sum_{r\in\mathfrak{R}} y_r \odot_{r\in\mathfrak{R}} \sum_{r\in\mathfrak{R}} w_r = \sum_{r\in\mathfrak{R}} y_r w_r$. Then integrating by parts again we arrive with,

$$\frac{d}{dt}\sum_{i=0}^{n}\int_\Omega n_i\left(\ln(\mathring{\kappa}_i n_i)+\mathring{\kappa}_i\right)dx + \sum_{i=0}^{n}\int_\Omega n_i^{-1}\mathscr{D}_i\nabla_x n_i\cdot\nabla_x n_i dx = \sum_{i=0}^{n}\int_\Omega m_i^{-1}\mathscr{A}_i(\mathring{n})\odot_{r\in\mathfrak{R}}\ln(n_i\mathring{\kappa}_i)dx. \tag{3.1}$$

For Ω bounded — which corresponds to the interesting case numerically — then using the fact that $a\ln a \leq 2e^{-1}\sqrt{a}$ for $0\leq a\leq 1$, we find that

$$\begin{aligned}\sum_{i=1}\int_\Omega n_i|\ln\mathring{\kappa}_i n_i|dx &= \sum_{i=1}^{n}\int_\Omega n_i\ln(\mathring{\kappa}_i n_i)dx - 2\sum_{i=1}^{n}\int_\Omega n_i\ln(\mathring{\kappa}_i n_i)\mathbb{1}_{0\leq\mathring{\kappa}_i n_i\leq 1}dx\\ &\leq \sum_{i=1}^{n}\int_\Omega n_i\ln(\mathring{\kappa}_i n_i)dx + 2(e\mathring{\kappa}_i)^{-1}|\Omega|.\end{aligned}$$

providing the weak form for (3.1):

$$\frac{d}{dt}\sum_{i=1}^{n}\int_\Omega n_i\left(|\ln\mathring{\kappa}_i n_i|+\mathring{\kappa}_i\right)dx + \sum_{i=1}^{n}\int_\Omega n_i^{-1}\mathscr{D}_i|\nabla_x n_i|^2\cdot\nabla_x n_i dx + \sum_{i=1}^{n}\int_\Omega m_i^{-1}\mathfrak{D}(\mathring{n})dx \leq \sum_{i=1}^{n}2(e\kappa_i)^{-1}|\Omega|,$$

where $|\nabla_x n_i|^2 = \nabla_x n_i\cdot\nabla_x n_i$.

The reaction term $\sum_i m_i^{-1}\mathfrak{D}(\mathring{n}) = -\Delta G$ behaves — up to a reference prefactor — as a scaled Gibbs free energy of the reactor system, since

$$\begin{aligned}\sum_{i=1}^{n} m_i^{-1}\mathfrak{D}(\mathring{n}) &= -\sum_{i=1}^{n} m_i^{-1}\mathscr{A}_i(\mathring{n})\odot_{r\in\mathfrak{R}}\ln\left(n_i\left[\prod_{r\in\mathfrak{R}}K_{eq,r}\right]^{-1/n(\sum_{r\in\mathfrak{R}}(\nu_{ir}^b-\nu_{ir}^f))}\right)\\ &= -\sum_{i=1}^{n} m_i^{-1}\mathscr{A}_i(\mathring{n})\odot_{r\in\mathfrak{R}}\left(\frac{1}{\sum_{r\in\mathfrak{R}}(\nu_{ir}^b-\nu_{ir}^f)}\right)\left(\ln n_i^{\sum_{r\in\mathfrak{R}}(\nu_{ir}^b-\nu_{ir}^f)} - n^{-1}\ln\prod_{r\in\mathfrak{R}}K_{eq,r}\right)\\ &= -\xi_r\odot_{r\in\mathfrak{R}}\sum_{r\in\mathfrak{R}}\ln K_{eq,r} - \sum_{r\in\mathfrak{R}}\left(k_{fr}\prod_{i=1}^{n}n_i^{\nu_{ir}^f} - k_{br}\prod_{i=1}^{n}n_i^{\nu_{ir}^b}\right)\odot_{r\in\mathfrak{R}}\ln Q(\mathring{n})\\ &= \xi_r\odot_{r\in\mathfrak{R}}\left(\ln Q(\mathring{n})+\Delta G^{\ominus}\right),\end{aligned} \tag{3.2}$$

where the reactor quotient $Q_r(\mathring{n})$ is given by:

$$Q(\mathring{n}) = \left(\prod_{i=1}^{n}\mathring{n}_i^{\sum_{r\in\mathfrak{R}}\nu_{ir}^b}\Big/\prod_{i=1}^{n}\mathring{n}_i^{\sum_{r\in\mathfrak{R}}\nu_{ir}^f}\right), \tag{3.3}$$

and where $\xi_r = \xi_r(t, \boldsymbol{x})$ is a reactor-scaled prefactor coefficient, and $\Delta G^{\ominus}$ the reference value. Thus, for spontaneous reactions it follows that $\Delta G \leq 0$. To make this precise notice that we may rewrite (3.2) as:

$$\begin{aligned}\sum_{i=1}^{n} m_i^{-1}\mathfrak{D}(\mathring{n}) &= -\sum_{i=1}^{n} m_i^{-1}\mathscr{A}_i(\mathring{n}) \odot_{r\in\mathfrak{R}} \ln\left(n_i\left(\prod_{r\in\mathfrak{R}} K_{eq,r}\right)^{-1/n(\sum_{r\in\mathfrak{R}}(\nu_{ir}^{b}-\nu_{ir}^{f}))}\right)\\ &= -\sum_{r\in\mathfrak{R}} k_{fr}\left(\prod_{i=1}^{n} n_i^{\nu_{ir}^{f}} - K_{eq,r}^{-1}\prod_{i=1}^{n} n_i^{\nu_{ir}^{b}}\right)\\ &\qquad \odot_{r\in\mathfrak{R}} \ln\left(\left(\prod_{r\in\mathfrak{R}} K_{eq,r}\right)^{-1}\prod_{i=1}^{n}\mathring{n}_i^{\sum_{r\in\mathfrak{R}}\nu_{ir}^{b}} \Big/ \prod_{i=1}^{n}\mathring{n}_i^{\sum_{r\in\mathfrak{R}}\nu_{ir}^{f}}\right)\\ &\geq 0.\end{aligned} \tag{3.4}$$

After some algebra it is clear that for each $r \in \mathfrak{R}$ we have a term of the form $(A-B)(\ln A - \ln B)$ such that the product is always positive.

As a consequence we obtain the scalar entropy $\mathscr{S}_{\mathfrak{R}} = \mathscr{S}_{\mathfrak{R}}(\mathring{n})$ over the reaction space $\mathfrak{R}$. That is, given bounded initial reaction state density $P_{0|r\in\mathfrak{R}}$ satisfying

$$P_{0|\forall r\in\mathfrak{R}} = \sum_{i=1}^{n}\int_{\Omega} \mathring{\kappa}_i n_i^0(|\ln n_i^0| + 1 + |x|)dx < \infty,$$

where $n_i^0 = n_{i|t=0}$ is the initial condition, summing over reactions $r \in \mathfrak{R}$ we obtain the following inequality on the system for any fixed n number of constituents over a bounded domain:

$$\begin{aligned}\mathscr{S}_{\mathfrak{R}} = \sup_{0\leq t\leq T}\Bigg\{&\sum_{i=1}^{n}\int_{\Omega} n_i(|\ln \mathring{\kappa}_i n_i| + \mathring{\kappa}_i)dx + \sum_{i=1}^{n}\int_0^t\int_{\Omega} m_i^{-1}\mathfrak{D}(\mathring{n})dxds\\ &+\sum_{i=1}^{n}\int_0^t\int_{\Omega} n_i^{-1}\mathscr{D}_i|\nabla_x n_i|^2 dxds\Bigg\} \leq P_{0|\forall r\in\mathfrak{R}} + \sum_{i=1}^{n} 2(e\mathring{\kappa}_i)^{-1}|\Omega| + C(T).\end{aligned} \tag{3.5}$$

where the first term on the left corresponds to the entropy contribution from the density of states, the second term on the left to the contribution from chemical energy production in the reactor, and the third on the left to the scattering entropy of the system. The constant $C(T)$ depends on the final state, unless reactor equilibrium is established for some $T_{eq} < T$, in which case C is a function of the equilibrium time $C(T_{eq})$.

§3.2 Consistent entropy and *p*-enrichment

The entropy relation derived above may be used to generate a local smoothness estimator on the solution of each cell's interior. Moreover, the entropy $\mathscr{S}_{\mathfrak{R}}$ is a particularly attractive functional due to the fact that first, it globally couples the n-components of the system, and also that it is a functional which approximates the local physical entropy of the solution, up to (2.10). In this way $\mathscr{S}_{\mathfrak{R}}$ provides for a natural way to test whether the full approximate solution (2.37) is entropy consistent (i.e. demonstrates bounded variation and dissipates at equilibrium). If it is entropy consistent, then it also may be used to determine where in Ω (i.e. which elements of Ω) the entropy demonstrates the most local variation.

In order to derive the global discrete total entropy $\mathscr{S}_{\mathfrak{R}}^{k+1}$ at any particular timestep t^{k+1}, we integrate in time such that for any discrete $t^{\ell} \in (0, t^{k+1}]$ we have:

$$\begin{aligned}\mathscr{S}_{\mathfrak{R}}^{k+1} = \sup_{0\leq t^{\ell}\leq t^{k+1}}\Bigg\{&\sum_{i=1}^{n}\int_{\Omega_{\mathcal{G}}} n_i^{\ell}(|\ln \mathring{\kappa}_i n^{\ell}|_i + \mathring{\kappa}_i)dx\\ &+\sum_{i=1}^{n}\int_0^{t^{k+1}}\int_{\Omega_{\mathcal{G}}} (n_i)^{-1}\mathscr{D}_i|\nabla_x n_i|^2 dxds\\ &+\sum_{i=1}^{n}\int_0^{t^{k+1}}\int_{\Omega_{\mathcal{G}}} m_i^{-1}\mathfrak{D}(\mathring{n})dxds\Bigg\} \leq P_{0|\forall r\in\mathfrak{R}} + \sum_{i=1}^{n} 2(e\mathring{\kappa}_i)^{-1}|\Omega| + C(T),\end{aligned} \tag{3.6}$$

where as above $\alpha_i^\ell = \alpha_{i|t=t^\ell}$.

For vanishing molar concentration the diffusivity coefficient may not vanish at a rate that captures the analytic behavior, so (3.6) in its implementational form becomes:

$$\begin{aligned}\mathscr{S}_{\mathfrak{R}}^{k+1} = \sup_{0\leq t^\ell\leq t^{k+1}} &\left(\sum_{i=1}^{n}\int_{\Omega_{\mathcal{G}}} n_i^\ell(|\ln \mathring{\kappa}_i n_i^\ell| + \mathring{\kappa}_i)dx\right)\\ &+\sum_{i=1}^{n}\int_0^{t^{k+1}}\int_{\Omega_{\mathcal{G}}} \mathbb{1}_{\{n_i\geq L\}}\left(\frac{\mathscr{D}_i}{n_i}\right)|\nabla_x n_i|^2 dxds\\ &+\sum_{i=1}^{n}\int_0^{t^{k+1}}\int_{\Omega_{\mathcal{G}}} m_i^{-1}\mathfrak{D}(\mathring{n})dxds \leq P_{0|\forall r\in\mathfrak{R}} + \sum_{i=1}^{n} 2(e\mathring{\kappa}_i)^{-1}|\Omega| + C(T),\end{aligned} \tag{3.7}$$

given some small positive constant $L\in\mathbb{R}^+$ where again $\mathbb{1}_{\{n_i\geq L\}}$ is the indicator function over the set containing $n_i \geq L$.

Similarly, we define the discrete local in $(t,\boldsymbol{x})$ entropy $\mathscr{S}_{\mathfrak{R},\Omega_{e_i}}^{k+1}$ by integrating over an element Ω_{e_i} restricted to t^{k+1} such that we obtain:

$$\begin{aligned}\mathscr{S}_{\mathfrak{R},\Omega_{e_i}}^{k+1} &= \sum_{i=1}^{n}\int_{\Omega_{e_i}} n_i^{k+1}(|\ln \mathring{\kappa}_i n_i^{k+1}| + \mathring{\kappa}_i)dx + \sum_{i=1}^{n}\int_{t^k}^{t^{k+1}}\int_{\Omega_{e_i}} m_i^{-1}\mathfrak{D}(\mathring{n})dxds\\ &+\sum_{i=1}^{n}\int_{t^k}^{t^{k+1}}\int_{\Omega_{e_i}} \mathbb{1}_{\{n_i\geq L\}}\left(\frac{\mathscr{D}_i}{n_i}\right)|\nabla_x n_i|^2 dxds,\end{aligned} \tag{3.8}$$

such that $n_i^{k+1} = n_{i|t=t^{k+1}}$. Then we proceed by defining the local in time change in entropy density $\Delta\hat{\rho}\mathscr{S}_{\mathfrak{R},\Omega_{e_i}}^{k+1}$ over $\text{int}(\Omega_{e_i})$ as satisfying:

$$\Delta\hat{\rho}\mathscr{S}_{\mathfrak{R},\Omega_{e_i}}^{k+1} = \hat{\rho}\left(\mathscr{S}_{\mathfrak{R},\Omega_{e_i}}^{k+1} - \mathscr{S}_{\mathfrak{R},\Omega_{e_i}}^{k}\right), \tag{3.9}$$

where the cell density is taken as $\hat{\rho} = |\Omega_{e_i}|^{-1}$.

We use equation (3.9) as an approximate measure of the variation in the local entropy with respect to a fixed volume elements (at timestep t^{k+1}) interior, $\text{int}(\Omega_{e_i})$. More explicitly, we use (3.9) as a local regularity estimator over the interior of Ω_{e_i} in order to develop a p-enrichment functional $\mathfrak{E}_i^{k+1} = \mathfrak{E}_i^{k+1}(\mathscr{P}^s(\Omega_{e_i}^{k+1}))$, which estimates the local internal energy of the element as an approximate measure of the local regularity of the solution. For $\mathscr{P}^{p_{\max}}(\Omega_{e_i})$ the maximum polynomial order allowed on any Ω_{e_i}, and $\mathscr{P}^s(\Omega_{e_i}^k)$ the present polynomial order, we define:

$$\mathfrak{E}_i^{k+1} = \begin{cases}\mathscr{P}^{s+1}(\Omega_{e_i}^{k+1}) & \text{if } \left(\left|\Delta\hat{\rho}\mathscr{S}_{\mathfrak{R},\Omega_{e_i}}^{k+1} - \Delta\varrho\mathscr{S}_{\mathfrak{R},\Omega_{e_i}}^{k+1}\right| \bowtie_{s+1} \mu_{s+1}\right)\wedge(s+1\leq p_{\max})\wedge(\tau_0\geq t^w),\\ \mathscr{P}^{s-1}(\Omega_{e_i}^{k+1}) & \text{if } \left(\left|\Delta\hat{\rho}\mathscr{S}_{\mathfrak{R},\Omega_{e_i}}^{k+1} - \Delta\varrho\mathscr{S}_{\mathfrak{R},\Omega_{e_i}}^{k+1}\right| \bowtie_{s-1} \mu_{s-1}\right)\wedge(s-1\geq p_{\min})\wedge(\tau_0\geq t^w),\end{cases} \tag{3.10}$$

where the change in the average global entropy density $\Delta\varrho\mathscr{S}_{\mathfrak{R}}^{k+1}$ at t^{k+1} is given by

$$\Delta\varrho\mathscr{S}_{\mathfrak{R}}^{k+1} = \varrho\left(\mathscr{S}_{\mathfrak{R}}^{k+1} - \mathscr{S}_{\mathfrak{R}}^{k}\right).$$

The notation $\bowtie_{\{\cdot\}}$ is simply a pair from the indefinite binary relations $\bowtie_{\{\cdot\}}\in\{<,>,\leq,\geq\}$ where the choice determines the difference between a Type I and and Type II enrichment scheme (see [60] for more details). Finally τ_0 is a counter that restricts the enriching/de-enriching so that it only occurs every $t^w\in\mathbb{N}$ timesteps.

The global entropy $\mathscr{S}_{\mathfrak{R}}^{k+1}$ at timestep t^{k+1} is defined fully in §3.3, and the global density is simply taken as $\varrho = |\Omega_{\mathcal{G}}|^{-1}$. The adjustable parameter $\mu_s = \mu(\iota_s)$ is a composite of the range of the entropy change at time t^{k+1} and a weight $\iota_s\in(0,1)$. That is the function may be written $\mu_{s+1} = \iota_{s+1}\delta$ over the midpoint of the range $\delta = \delta(\hat{\rho}, \mathscr{S}_{\mathfrak{R},\Omega_{e_i}}^{k}, \mathscr{S}_{\mathfrak{R},\Omega_{e_i}}^{k+1})$ of the change in entropy density

$$\delta = \max_i \Delta\hat{\rho}\mathscr{S}_{\mathfrak{R},\Omega_{e_i}}^{k+1} - \min_i \Delta\hat{\rho}\mathscr{S}_{\mathfrak{R},\Omega_{e_i}}^{k+1}.$$

Clearly (3.10) has the effect of using the variation in the entropy change locally to weight some fraction of the cells for p-enrichment and the rest for p-de-enrichment, depending only on how far their relative local change in entropy lies from the median of the range.

In contrast to alternative choices for p-enrichment, this scheme provides for a cogent physical interpretation that serves as support for the enrichment strategy. Namely, we see that in areas in which the relative disorder (i.e. the relative entropy) of a cell exceeds a specified allowed variation within the cell itself, then we de-enrich/enrich our solution, thus avoiding potential instabilities, while drawing out relevant physical features of the solution. Likewise in areas of relative order (or stable smoother regions) we may readily enrich/de-enrich our solution, up to the type of scheme we implement.

More precisely, this choice of enrichment and de-enrichment occurs while maintaining the "stabilizing center" of dioristic schemes. In this sense (3.10) is a dioristic entropy scheme (for a general introduction to Type I and Type II dioristic schemes and their stability properties see [60]). To make this explicit, denoting the global average change in entropy density by $\mathrm{Avg}_{\Omega_{\mathcal{G}}}\Delta\hat{\rho}\mathscr{S}^{k+1}_{\mathfrak{R},\Omega_{e_i}}$, the "stabilizing center" at timestep $k+1$ is the discrete subdomain $\mathfrak{c} \subseteq \Omega_{hp}$ comprised of the union of elements over which the change in entropy density satisfies the condition,

$$\mathfrak{c} = \left\{ \bigcup_{1\leq j\leq ne} \Omega_{e_j} : \left|\Delta\hat{\rho}\mathscr{S}^{k+1}_{\mathfrak{R},\Omega_{e_i}} - \mathrm{Avg}_{\Omega_{\mathcal{G}}}\Delta\hat{\rho}\mathscr{S}^{k+1}_{\mathfrak{R},\Omega_{e_i}}\right| \bowtie_s \mu_s,\ \forall i \right\}. \tag{3.11}$$

Note that μ_s in (3.10) can itself represent a range when $\mu_{s+1} \neq \mu_{s-1}$, in which case $\mathfrak{c}$ can become disjoint. As discussed in [60], this stabilizing center is the minimal set over which the stability setting of the solution should be chosen, in order to expect convergent behavior. It turns out that understanding this relationship between the stabilizing center $\mathfrak{c}$ and the restriction τ_0 ultimately exemplifies the central nuance at play in both practical applications as well as convergence studies (see §4 for more details).

We have also tested enrichment strategies based on slightly more abstract principles. For example, one may simply choose a fraction of elements with respect to the magnitude of their relative change in entropy density, or with respect to $|\Delta\hat{\rho}\mathscr{S}^{k+1}_{\mathfrak{R},\Omega_{e_i}} - \Delta\varrho\mathscr{S}^{k+1}_{\mathfrak{R},\Omega_{e_i}}|$ by cell. Likewise, when using a hierarchical basis one may use the scheme described in [60] to measure the perturbative variation in the higher terms with respect to the L^q–norm. Many of these alternative strategies can lead to stable schemes that effectively "sense" relative energy fluctuations with respect the Δt. However, it should be noted as a word of caution that (3.10) is particularly well-suited for naturally avoiding the observed phenomenon of bunching in the local variational space. This bunching of the solution often leads to a flickering of enrichment/coarsening of a substantial number of elements taking values close to the "center" of the chosen discriminating parameter (e.g. $|\Delta\rho\mathscr{S}^{k+1}_{\mathfrak{R},\Omega_{e_i}} - \Delta\varrho\mathscr{S}^{k+1}_{\mathfrak{R},\Omega_{e_i}}|$ in (3.10)). This behavior is a potential source of debilitating inefficiency in the scheme, and can be difficult to isolate without recourse to an entropy-type formalism.

§3.3 The entropic jump and *hp*-adaptivity

As already discussed, the global entropy formulation from §3.1 is predicated over a compact space Ω, while in general we are interested in more complicated boundary formulations, in particular any boundary condition satisfying (2.12). In this more general setting we see that equation (3.5) by way of the divergence theorem becomes,

$$\begin{aligned}\mathscr{S}_{\mathfrak{R}} = \sup_{0\leq t\leq T} \Bigg\{ &\sum_{i=1}^{n}\int_{\Omega} n_i(|\ln \mathring{\kappa}_i n_i| + \mathring{\kappa}_i)dx + \sum_{i=1}^{n}\int_0^t\int_{\Omega} m_i^{-1}\mathfrak{D}(\mathring{n})dxds \\ &\sum_{i=1}^{n}\int_0^t\int_{\Omega} n_i^{-1}\mathscr{D}_i|\nabla_x n_i|^2 dxds\Bigg\} \\ \leq P_{0|\forall r\in\mathfrak{R}} &+ \sum_{i=1}^{n} 2(e\mathring{\kappa}_i)^{-1}|\Omega| + C(T) + \sum_{i=1}^{n}\int_0^t\int_{\partial\Omega}(\ln(n_i\mathring{\kappa}_i) + \mathring{\kappa}_i + 1)\mathscr{D}_i\nabla_x n_i\cdot\boldsymbol{n}dSds.\end{aligned} \tag{3.12}$$

Thus, as before, the discrete approximation to (3.12) simply yields,

$$\begin{aligned}\mathscr{S}_{\mathfrak{R}}^{k+1} = &\sup_{0\le t^{\ell}\le t^{k+1}}\left(\sum_{i=1}^{n}\int_{\Omega_{\mathcal{G}}} n_i^{\ell}(|\ln \mathring{\kappa}_i n_i^{\ell}| + \mathring{\kappa}_i)dx\right)\\ &+\sum_{i=1}^{n}\int_0^{t^{k+1}}\int_{\Omega_{\mathcal{G}}} \mathbb{1}_{\{n_i\ge L\}}\left(\frac{\mathscr{D}_i}{n_i}\right)|\nabla_x n_i|^2 dxds\\ &+\sum_{i=1}^{n}\int_0^{t^{k+1}}\int_{\Omega_{\mathcal{G}}} m_i^{-1}\mathfrak{D}(\mathring{n})dxds \le P_{0|\forall r\in\mathfrak{R}} + \sum_{i=1}^{n} 2(e\mathring{\kappa}_i)^{-1}|\Omega| + C(T)\\ &+\sum_{i=1}^{n}\int_0^{t^{k+1}}\int_{\partial\Omega_{\mathcal{G}}} \mathbb{1}_{\{n_i\ge L\}}(\ln(n_i\mathring{\kappa}_i) + \mathring{\kappa}_i + 1)\mathscr{D}_i\nabla_x n_i\cdot\boldsymbol{n}dSds.\end{aligned} \tag{3.13}$$

Now, in the local approximation it is clear enough how to reformulate (3.13) over cells such that we obtain a local approximation to the entropy in the neighborhood of a particular cell. However, for the case of h-adaptivity we are more directly concerned with the local jump in entropy across the face of neighboring cells, since it is these jumps that serve as a proper diagnostic probe for stable hp-adaptivity (e.g. see [7, 25, 26, 54]). Thus we define the local entropic jump $\mathscr{J}_{\mathfrak{R},\Omega_{e_i}}^{k+1}$ at time t^{k+1} by

$$\mathscr{J}_{\mathfrak{R},\Omega_{e_i}}^{k+1} = \sum_{i=1}^{n}\int_0^{t^{k+1}}\int_{\partial\Omega_{e_i}} \mathbb{1}_{\{n_i\ge L\}}(\ln(n_i\mathring{\kappa}_i) + \mathring{\kappa}_i + 1)\mathscr{D}_i\nabla_x n_i\cdot\boldsymbol{n}dSds, \tag{3.14}$$

such that the density of the variation in the entropic jump $\rho\Delta\mathscr{J}_{\mathfrak{R},\Omega_{e_i}}^{k+1}$ is given to satisfy

$$\hat{\rho}\Delta\mathscr{J}_{\mathfrak{R},\Omega_{e_i}}^{k+1} = \hat{\rho}\left(\mathscr{J}_{\mathfrak{R},\Omega_{e_i}}^{k+1} - \mathscr{J}_{\mathfrak{R},\Omega_{e_i}}^{k}\right). \tag{3.15}$$

We proceed by estimating the approximate flux of the internal energy of the system by constructing the h-adaptivity functional $\mathfrak{A} = \mathfrak{A}(\mathscr{T}_{h'}(\Omega_{e_i}^{k+1}))$ where the mesh triangulation $\mathscr{T}_h$ at time t^k given by $h = h(t^k, \boldsymbol{x})$ is refined to level $h' = h(t^{k+1}, \boldsymbol{x})$ — that is, we isotropically refine to $h/2$ in each spatial dimension — over cell Ω_{e_i} at time t^{k+1}. Similarly we may unrefine $\mathfrak{A}_i^{k+1} = \mathfrak{A}(\mathscr{T}_{h_0}(\Omega_{e_i}^{k+1}))$ to level $h_0 = h(t^{k+1}, \boldsymbol{x})$, which is to isotropically coarsen to $2h$ in each spatial dimension.

For example, in dimension $N = 2$ the refinement would take a quadrilateral parent cell Ω_{e_i} and split it into four child cells $\mathcal{C}_j$, while a coarsening would take four child cells denoted $\mathcal{C}_j$ and merge them into a single parent element Ω_{e_i}. Thus depending on the evaluation of $\mathfrak{A}$, we obtain the full h-adaptivity functional:

$$\mathfrak{A}_i^{k+1} = \begin{cases}\mathscr{T}_{h'}(\Omega_{e_i}^{k+1}) & \text{if } \left(\left|\hat{\rho}\Delta\mathscr{J}_{\mathfrak{R},\Omega_{e_i}}^{k+1} - \varrho\Delta\mathscr{J}_{\mathfrak{R}}^{k+1}\right| \bowtie_{h'} \eta_{h'}\right)\wedge(s+1\le h_{\max})\wedge(\tau_0\ge t^w),\\ \mathscr{T}_{h_0}(\Omega_{e_i}^{k+1}) & \text{if } \left(\left|\hat{\rho}\Delta\mathscr{J}_{\mathfrak{R},\Omega_{e_i}}^{k+1} - \varrho\bar{\Delta}\mathscr{J}_{\mathfrak{R}}^{k+1}\right| \bowtie_{h'} \eta_{h_0}\right)\wedge(s-1\ge h_{\min})\wedge(\tau_0\ge t^w)\ \forall\mathcal{C}_j,\end{cases} \tag{3.16}$$

where $h_{\max}$ and $h_{\min}$ correspond to the maximum and minimum refinement levels, respectively. Here again, the density of the global change in the entropic jump is given such that:

$$\varrho\Delta\mathscr{J}_{\mathfrak{R}}^{k+1} = \varrho\left(\mathscr{J}_{\mathfrak{R}}^{k+1} - \mathscr{J}_{\mathfrak{R}}^{k}\right),$$

where ϱ is the same as in §3.2. Also as in §3.2, the adjustable parameter $\eta_h = \eta(\upsilon_h)$ is again defined over the range of the change in the entropic jump $\psi = \psi(\rho, \mathscr{J}_{\mathfrak{R},\Omega_{e_i}}^{k}, \mathscr{J}_{\mathfrak{R},\Omega_{e_i}}^{k+1})$, and is given by $\eta_h = \upsilon_h\psi$ such that

$$\psi = \max_i \rho\Delta\mathscr{J}_{\mathfrak{R},\Omega_{e_i}}^{k+1} - \min_i \rho\mathscr{J}_{\mathfrak{R},\Omega_{e_i}}^{k+1},$$

and $\upsilon_h \in (0, 1)$. The remaining notation $\bowtie_{\{\cdot\}}, \tau_0$, and t^w are given as in §3.2.

It is further interesting to note that the local change in the entropic jump $\Delta\mathscr{J}_{\mathfrak{R},\Omega_{e_i}}^{k+1}$ is independent of the reaction entropy at time level t^k, and ends up depending only on the reaction coupling from the earlier timesteps as well as on the present states effective local scattering. That being said, it is clear that just as (3.10) in §3.2

effectively p-enriches the solution based on the local physics of the system, here, we find that (3.16) has the effect of flagging elements with a high/low relative change in their entropic jumps for h-refinement, and those with low/high relative change in their entropic jumps for h-coarsening. That is, in areas where the entropy is changing dramatically across the elements boundary, we may, depending on our regime, either refine or coarsen. However, we are also presented with the additional constraint denoted: $\forall \mathcal{C}_j$. The meaning of $\forall \mathcal{C}_j$ here is that in order to actually coarsen a parent element Ω_{e_i} comprised of j children elements $\cup_j \mathcal{C}_j = \Omega_{e_i}$, each child $\mathcal{C}_j$ must be independently flagged for coarsening. In other words, all children of an isotropically refined element Ω_{e_i} must contain a coarsen flag at time level $k+1$ in order for the parent cell to ultimately be refined at time level $k+1$. For more details on this isotropic refinement strategy we direct the reader to [7].

Finally, we couple the h-adaptivity functional $\mathfrak{A}_i^{k+1}$ to the p-enrichment functional $\mathfrak{E}_i^{k+1}$ such that h-adaptivity is always preferentially chosen over p-enrichment. That is, clearly the cell localized entropy $\mathscr{S}_{\mathfrak{R},\Omega_{e_i}}^{k+1}$ and its corresponding entropic jump $\mathscr{J}_{\mathfrak{R},\Omega_{e_i}}^{k+1}$ are strongly coupled by virtue of (2.11), but in order to avoid numerical instabilities caused by erroneously p-enriching relatively inert cells experiencing high entropic fluxes entering through neighboring faces, we evaluate the simple kinetic switch functional $\mathfrak{K}_i^{k+1} = \mathfrak{K}_i^{k+1}(\mathfrak{A}_i^{k+1}, \mathfrak{E}_i^{k+1})$ determined by evaluating:

$$\mathfrak{K}_i^{k+1} = \begin{cases} \mathfrak{A}_i^{k+1} \wedge \mathfrak{E}_i^{k+1} & \text{if } \mathscr{T}_{h'}(\Omega_{e_i}^{k+1}) \wedge \mathscr{P}^{s}(\Omega_{e_i}^{k+1}) \wedge \mathscr{S}_{\mathfrak{R}}^{k+1}, \\ \mathfrak{A}_i^{k+1} & \text{if } \mathscr{T}_{h'}(\Omega_{e_i}^{k+1}) \wedge \mathscr{P}^{s+1}(\Omega_{e_i}^{k+1}) \wedge \mathscr{S}_{\mathfrak{R}}^{k+1}, \\ \mathfrak{A}_i^{k+1} \wedge \mathfrak{E}_i^{k+1} & \text{if } \mathscr{T}_{h_0}(\Omega_{e_i}^{k+1}) \wedge \mathscr{P}^{s}(\Omega_{e_i}^{k+1}) \wedge \mathscr{S}_{\mathfrak{R}}^{k+1}, \\ \mathfrak{A}_i^{k+1} \wedge \mathfrak{E}_i^{k+1} & \text{if } \mathscr{T}_{h_0}(\Omega_{e_i}^{k+1}) \wedge \mathscr{P}^{s+1}(\Omega_{e_i}^{k+1}) \wedge \mathscr{S}_{\mathfrak{R}}^{k+1}, \\ 0 & \text{otherwise}, \end{cases} \tag{3.17}$$

whereby we are able to stabilize these spurious quiescent instabilities, and yet still enforce the entropy consistency of the scheme.

§4 Example Applications

§4.1 Error behavior at equilibrium

Let us now consider a simple equilibrium problem with vanishing mass diffusivity coefficient $\mathscr{D}_i$ comprised of the two chemical species $\mathfrak{M}_1$ and $\mathfrak{M}_2$, and constructed in such a way as to allow for complete decoupling between the constituents in the mass action.

That is, consider the elementary equilibrium reaction satisfying:

$$\nu_1^f \mathfrak{M}_1 \underset{k_b}{\overset{k_f}{\rightleftharpoons}} \nu_2^b \mathfrak{M}_2 \tag{4.1}$$

such that the coupled system of differential equations is comprised of,

$$\rho_1' = m_1 \nu_1^f (k_b n_2^{\nu_1^b} - k_f n_1^{\nu_1^f}), \quad \rho_2' = m_2 \nu_2^b (k_f n_1^{\nu_1^f} - k_b n_2^{\nu_1^b}), \quad \text{so that } m_2 \nu_2^b \rho_1' = -m_1 \nu_1^f \rho_2'. \tag{4.2}$$

Integrating for any $t \in [0, T_{eq})$ with T_{eq} the equilibrium time (which exists *a priori* for $\min\{k_b, k_f\} \neq 0$) and letting the initial concentration $n_{2,0} = 0$, then we further notice that at each t we have

$$n_1(t) = n_{1,0} - \left(\frac{m_1 \nu_1^f}{m_2 \nu_2^b}\right) n_2(t), \quad \text{and at equilibrium that } \; n_1(T_{eq}) = n_{1,0} - \left(\frac{m_1 \nu_1^f}{m_2 \nu_2^b}\right) n_2(T_{eq}). \tag{4.3}$$

By mass conservation $m_1 \nu_2^b = m_2 \nu_2^b$ and assuming the ideal behavior $K_{eq} = k_f / k_b = n_2(T_{eq}) / n_1(T_{eq})$, where (4.3) provide that $n_2 = n_{1,0} - n_1(t)$, and also yields for the equilibrium constant that $K_{eq} = (n_{1,0} - n_1(T_{eq}))/n_1(T_{eq})$. Using these relations, we then rewrite n_1' in the first equation of (4.2) as

$$\begin{aligned} n_1' &= k_b n_2 - k_f n_1 \\ &= k_b n_{1,0} - (k_b + k_f) n_1 \\ &= (k_f + k_b)(n_1(T_{eq}) - n_1). \end{aligned} \tag{4.4}$$

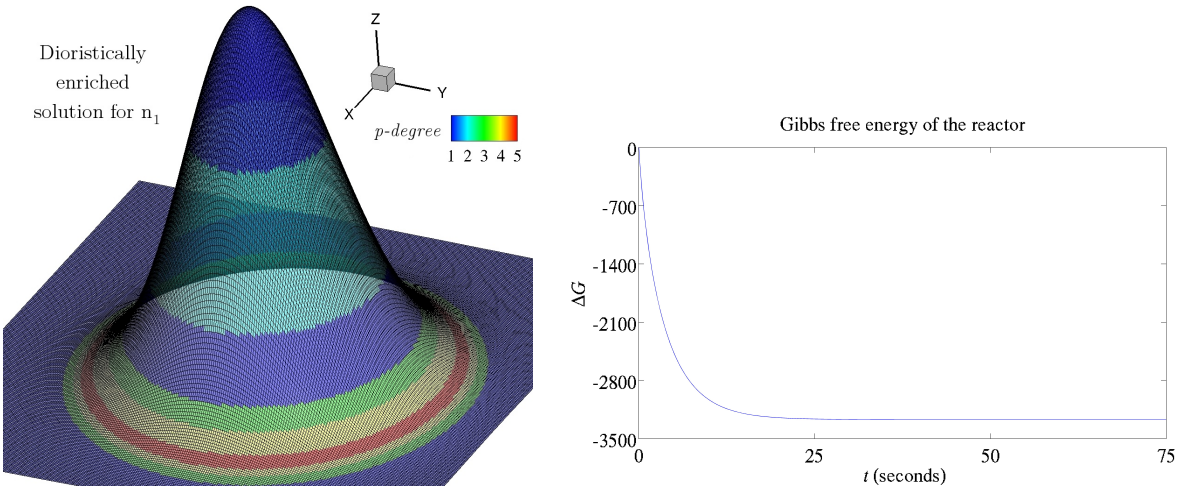

Figure 3: On the left, the type I dioristic entropy p-enrichment scheme for $h = 10/128$, $\Delta t = 0.1$, RKC(2,2), $\epsilon = 2/13$, $\iota_{s+1} = \iota_{s-1} = 0.15$, fstep $= 5$ $p_{low} = 1$ and $p_{high} = 5$ after six timesteps with $t^w = 0$. On the right, the Gibbs free energy of the reaction, $\Delta t = 0.05$, $T = 75$ seconds, $p = 1$.

Recall that for an ODE in ϖ of the form $\varpi' = C_1\varpi + C_2$ we can write the general solution over Δt by,

$$\varpi(t^{n+1}) = \exp^{\int_{\Delta t} C_1 dt}\left(\varpi(t^n) + \frac{C_2}{C_1}\right) - \frac{C_2}{C_1}. \tag{4.5}$$

Thus for (4.4) we can write that

$$n_1 = \exp^{-\int_{\mathfrak{X}}(k_f+k_b)ds}\left(n_{1,0} - n_1(T_{eq})\right) + n_1(T_{eq}). \tag{4.6}$$

for any $\mathfrak{X} \subset [0, T_{eq})$ containing the initial state and any $t \geq T_{eq}$, which is just to say the solution only depends upon the initial and equilibrium concentration of α_1 — hence fully independent of α_2.

Then to test our p-enrichment method from §3.2 we compare the error behavior of (4.6) against p using our approximate strategy from §2.4. We set this up by solving for (4.6) at an endtime that is within machine precision to the equilibrium asymptotics, which we denote as the approximate equilibrium state $T_{eq,h}$. Since this equilibrium state is arrived at by way of (4.2), we must compare our results to the top order solution, which here is determined at polynomial degree $p = 5$.

Given our initial state, we find that $T_{eq,h} \leq T \geq 4.17$ minutes is sufficient for convergence to approximate equilibrium. Here we have a stable equilibrium solution (for example, see definition 11.21 in [76]), using the following initial conditions:

$$n_{1,0} = 1 + \tfrac{4}{5}e^{-15(\boldsymbol{x}-\frac{1}{2})^2/4}, \quad \text{and} \quad n_{2,0} = 0,$$

which can be physically motivated as projecting a localized chemical plume in some solvent. We test each time-stepping regime separately, as shown in Table 1. It is worth noting that the time it takes the RKC solution to reach $T_{eq,h}$ is longer than the time it takes the SSP solution to reach $T_{eq,h}$. This observation is in agreement with previous work [83, 85], where the expanded stability region recovers real eigenmodes of the solutions that fluctuate about the equilibrium state more readily, while the SSP scheme rapidly dampens them. Similar effects are seen in the implicit (IMEX) solution depending on the solver controls set in the Newton-Krylov method, which in our cases are quite low, where both the GMRES and Newton tolerances are set to 10^{-10}. In figure 3 we show the basic behavior of the p–enrichment algorithm when employing the type I dioristic strategy. As is clear from the spatial graph, the p level is highest in areas of greatest curvature, and lowest in areas of lowest curvature along the reacting gaussian conditions. Moreover, as discussed in §3, figure 3 demonstrates that while performing p-enrichment on (4.2) the solution smoothly preserves the second law of thermodynamics.

	IMEX			RKC, $\epsilon = 2/13$			RKSSP(2,2)		
p	L^2-error	ι_{s-1}	t^w	L^2-error	ι_{s-1}	t^w	L^2-error	ι_{s-1}	t^w
5	–	–	–	–	–	–	–	–	–
4	1.1653×10^{-6}	–	–	1.2095×10^{-6}	–	–	1.1653×10^{-6}	–	–
3	2.39862×10^{-5}	–	–	2.48957×10^{-5}	–	–	2.39862×10^{-5}	–	–
2	0.0004464014	–	–	0.0004633258	–	–	0.0004464013	–	–
1	0.0073297268	–	–	0.0076076191	–	–	0.0073297269	–	–
1–2	0.0035749629	0.8	50	0.0040011919	0.8	50	0.0034345233	0.8	50
2–3	8.89191×10^{-5}	0.8	50	0.0001170498	0.8	50	8.89190×10^{-5}	0.8	50
3–4	1.29605×10^{-5}	0.8	50	1.25154×10^{-5}	0.8	50	1.08873×10^{-5}	0.8	50
4–5	2.75041×10^{-7}	0.8	50	3.662×10^{-7}	0.8	50	2.75040×10^{-7}	0.8	50

Table 1: We give the L^2-errors for the p-enrichment scheme, as discussed in §3.2. Here we have set $\iota_{s+1} = 0.0$, with $\Delta t = .3$ seconds, $h = 1/32$ and $T = 30$ seconds.

§4.2 Three-dimensional Lotka-Volterra reaction–diffusion

§4.2.1 An exact solution

Though the generalized Lotka-Volterra system frequently finds application in population dynamics, the general mathematical form of the system actually admits all chemical reactions with mass action of the form $\mathscr{A}_i$ from (2.11). For a generalized Lotka-Volterra (GLV) system [14, 15] with mass diffusion corresponding to (2.11), we mean a solution to any system obeying the following general equation:

$$\left.\begin{aligned} &\partial_t \rho_i - \nabla_x \cdot (\mathscr{D}_i \nabla_x \rho_i) - \mathscr{L}_i(\mathring{n}) = 0 \\ &\mathscr{L}_i(\mathring{n}) = \breve{\lambda}_i n_i + n_i \textstyle\sum_{j=1}^n A_{ij} \prod_{k=1}^n n_k^{B_{jk}} \end{aligned}\right\} \text{ GLV system,} \tag{4.7}$$

where $\breve{\lambda}_i$ is a real or complex parameter and B and A are real or complex valued square matrices. Clearly any equation satisfying (2.11) satisfies (4.7), as $\mathscr{A}_i$ is a special form of $\mathscr{L}_i$. In particular we can restrict to the standard Lotka–Volterra (LV) [17, 46] system of order n wherein $\mathscr{L}_i$ reduces to $\mathscr{L}_i(\mathring{n}) = \breve{\lambda}_i n_i + n_i \sum_{j=1}^n A_{ij} n_j$, which is then a formal subsystem of the mass action from (2.11).

Then we first consider an exact case when $n = 3$ corresponds to three chemical species, and the mass diffusion vanishes. It turns out that any chemical equation satisfying (2.13) that splits over the mass action in its components to satisfy,

$$\begin{gathered} \frac{d\rho_1}{dt} = \mathscr{N}_1 n_1 + \mathscr{U}_1 n_1^2 + \mathscr{O}_{12} n_1 n_2 + \mathscr{O}_{13} n_1 n_3, \quad \frac{d\rho_2}{dt} = \mathscr{N}_2 n_2 + \mathscr{O}_{21} n_2 n_1 + \mathscr{U}_2 n_2^2 + \mathscr{O}_{23} n_2 n_3, \\ \frac{d\rho_3}{dt} = \mathscr{N}_3 n_3 + \mathscr{O}_{31} n_3 n_1 + \mathscr{O}_{32} n_3 n_2 + \mathscr{U}_3 n_3^2, \end{gathered} \tag{4.8}$$

where the constants are given by,

$$\mathscr{N}_i = m_i \sum_{r \in \mathfrak{R}} (\nu_{ir}^b - \nu_{ir}^f) \left(\mathbb{1}_{\{\nu_{ir}^f > 0\}} k_{fr} - \mathbb{1}_{\{\nu_{ir}^b > 0\}} k_{br} \right), \mathscr{U}_i = m_i \sum_{r \in \mathfrak{R}} (\nu_{ir}^b - \nu_{ir}^f) \left(\mathbb{1}_{\{\nu_{ir}^f > 1\}} k_{fr} - \mathbb{1}_{\{\nu_{ir}^b > 1\}} k_{br} \right),$$
$$\mathscr{O}_{ij} = m_i \sum_{r \in \mathfrak{R}} (\nu_{ir}^b - \nu_{ir}^f) \left(\mathbb{1}_{\{\nu_{ir}^f, \nu_{jr}^f > 0\}} k_{fr} - \mathbb{1}_{\{\nu_{ir}^b, \nu_{jr}^b > 0\}} k_{br} \right),$$

is nothing but a three-dimensional standard Lotka-Volterra (LV) chemical system (note that swapping out a chemical species n_i for a population density x_i recovers the corresponding biological models).

Now, in order to restrict to a subsystem that is directly solvable by way of the Prelle-Singer algorithm, we choose that: $\mathscr{U}_1 m_1^{-1} = \mathscr{O}_{21} m_2^{-1} = \mathscr{O}_{31} m_3^{-1}$, $\mathscr{O}_{12} m_1^{-1} = \mathscr{U}_2 m_2^{-1} = \mathscr{O}_{32} m_3^{-1}$, and $\mathscr{O}_{13} m_1^{-1} = \mathscr{O}_{23} m_2^{-1} = \mathscr{U}_3 m_3^{-1}$,

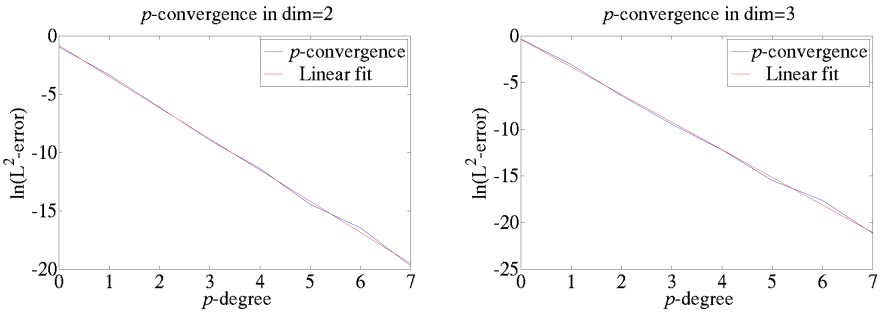

Figure 4: We plot the p-convergence of ρ_1, where in $N = 2$ we set $h/10 = 1/32$ and for $N = 3$ we have $h/10 = 1/16$.

p	L^2-error for $N = 2$, $h/10 = 32$	L^2-error for $N = 3$, $h/10 = 16$
0	0.390926632369	0.720254910486
1	0.035884566508	0.047256483871
2	0.002221513109	0.001666469980
3	0.000132690544	7.8824913×10^{-5}
4	1.1521953×10^{-5}	5.001097×10^{-6}
5	5.38640×10^{-7}	1.88819×10^{-7}
6	7.1314×10^{-8}	2.2219×10^{-8}
7	2.749×10^{-9}	6.49×10^{-10}

Table 2: We give the L^2-errors for ρ_1 shown in Figure 4.

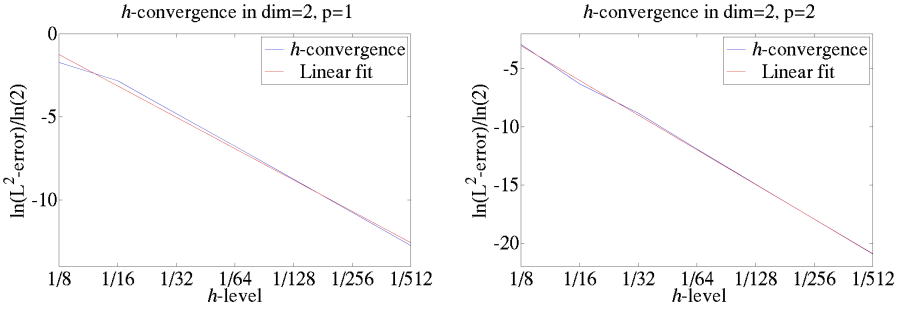

Figure 5: The h-convergence of ρ_1 with $N = 2$, where the h-levels are defined as the $h/10$ values here and below.

so that the $\mathscr{N}_i$'s are the remaining parameters in (4.8). As a consequence we arrive at a directly solvable solution. Then for the $\mathfrak{N}_i$'s being any excess/bulk/bath constituents, a reactor system comprised of ten coupled reactions that satisfies this equation is:

$$\begin{gathered}
\mathfrak{M}_1 + \mathfrak{M}_2 \xrightarrow{k_{f_1}} 2\mathfrak{M}_2, \quad \mathfrak{M}_1 + \mathfrak{M}_3 \xrightarrow{k_{f_2}} 3\mathfrak{M}_3, \quad 2\mathfrak{M}_1 + \mathfrak{N}_1 \xrightarrow{k_{f_3}} 3\mathfrak{M}_1, \\
\mathfrak{M}_2 + \mathfrak{M}_3 + \mathfrak{N}_2 \xrightarrow{k_{f_4}} 2\mathfrak{M}_2, \quad 2\mathfrak{M}_2 + \mathfrak{N}_3 \xrightarrow{k_{f_5}} \mathfrak{M}_2 + \mathfrak{N}_4, \quad \mathfrak{M}_1 + \mathfrak{M}_3 \xrightarrow{k_{f_6}} 3\mathfrak{M}_1, \\
2\mathfrak{M}_3 + \mathfrak{N}_5 \xrightarrow{k_{f_7}} 3\mathfrak{M}_3, \quad \nu^f_{18}\mathfrak{M}_1 \xrightarrow{k_{f_8}} \mathfrak{N}_4, \quad \nu^f_{29}\mathfrak{M}_2 \xrightarrow{k_{f_9}} \mathfrak{N}_5, \quad \nu^f_{310}\mathfrak{M}_3 \xrightarrow{k_{f_{10}}} \mathfrak{N}_6.
\end{gathered} \tag{4.9}$$

Since the bulk concentrations $[\mathfrak{N}_i]$ are treated as constant, this just means that the system is constrained by, $[\mathfrak{N}_1]k_{f_3} = k_{f_1} = 2k_{f_2} - k_{f_6}$, $k_{f_1} = -[\mathfrak{N}_3]k_{f_5} = -[\mathfrak{N}_2]k_{f_4}$, and $2k_{f_6} - k_{f_2} = [\mathfrak{N}_2]k_{f_4} = [\mathfrak{N}_5]k_{f_7}$.

	$p=1$		$p=2$	
$h/10$	L^2-error	Convergence Rate	L^2-error	Convergence Rate
1/8	0.303458180745	–	0.133322131328	–
1/16	0.141502142646	1.10*	0.012682532556	3.39*
1/32	0.035884566508	1.98	0.002221513109	2.51*
1/64	0.009246598384	1.96	0.000261196771	3.08
1/128	0.002327152982	1.99	3.2121273×10^{-5}	3.02
1/256	0.000582524118	2.00	3.991183×10^{-6}	3.00
1/512	0.0001456459723	2.00	4.97756×10^{-7}	3.00

Table 3: We give the L^2-errors and convergence rates shown in Figures 6 for $N=2$, where * indicates preasymptotic behavior.

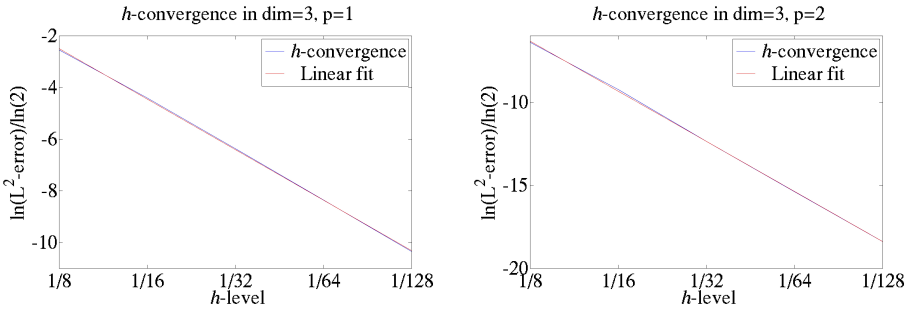

Figure 6: Here we show the h-convergence of the equilibrium solution, where $p=1$ and $p=2$ in $N=3$. Again the h-levels are the $h/10$ values.

	$p=1$		$p=2$	
$h/10$	L^2-error	Convergence Rate	L^2-error	Convergence Rate
1/8	0.171572963681	—	0.011957122768	—
1/16	0.047256483871	1.78	0.001666469980	2.72
1/32	0.012136203507	1.94	0.000190814465829426	2.93
1/64	0.00305803251442433	1.98	2.33630735758859e-05	2.98
1/128	0.000766609126530302	2.00	2.90899193162474e-06	3.00

Table 4: We give the L^2-errors and convergence rates shown in Figure 5 for $N=3$.

The modified Prelle-Singer algorithm applied to this system provides the following integrals of motion I_j (as explicitly derived in [20]):

$$I_1 = \left(\frac{n_3 e^{(\mathscr{N}_2 m_2^{-1} - \mathscr{N}_3 m_3^{-1})t}}{n_2}\right), \quad I_2 = \left(\frac{n_3 e^{(\mathscr{N}_1 m_1^{-1} - \mathscr{N}_3 m_3^{-1})t}}{n_1}\right),$$
$$I_3 = \left(\frac{(m_1 m_2 m_3)^{-1} e^{\mathscr{N}_1 m_1^{-1} t}(\mathscr{N}_1\mathscr{N}_2\mathscr{N}_3 + n_1\mathscr{N}_2\mathscr{N}_3\mathscr{U}_1 + n_2\mathscr{N}_1\mathscr{N}_3\mathscr{U}_2 + n_3\mathscr{N}_1\mathscr{N}_2\mathscr{U}_3)}{n_1}\right).$$

This leads to a fully coupled locally integrable mass action along the splitting discussed in §2, which is the

following time-dependent solution to (4.8):

$$
\begin{aligned}
n_1 &= \left(\frac{I_1 \mathscr{N}_1 \mathscr{N}_2 \mathscr{N}_3 e^{\mathscr{N}_1 m_1^{-1} t}}{I_3 I_1 - (I_1 \mathscr{U}_1 \mathscr{N}_2 \mathscr{N}_3 e^{\mathscr{N}_1 m_1^{-1} t} + I_2 \mathscr{U}_2 \mathscr{N}_1 \mathscr{N}_3 e^{\mathscr{N}_2 m_2^{-1} t} + I_1 I_2 \mathscr{U}_3 \mathscr{N}_1 \mathscr{N}_2 e^{\mathscr{N}_3 m_3^{-1} t})} \right), \\
n_2 &= \left(\frac{I_2 \mathscr{N}_1 \mathscr{N}_2 \mathscr{N}_3 e^{\mathscr{N}_2 m_2^{-1} t}}{I_3 I_1 - (I_1 \mathscr{U}_1 \mathscr{N}_2 \mathscr{N}_3 e^{\mathscr{N}_1 m_1^{-1} t} + I_2 \mathscr{U}_2 \mathscr{N}_1 \mathscr{N}_3 e^{\mathscr{N}_2 m_2^{-1} t} + I_1 I_2 \mathscr{U}_3 \mathscr{N}_1 \mathscr{N}_2 e^{\mathscr{N}_3 m_3^{-1} t})} \right), \\
n_3 &= \left(\frac{I_1 I_2 \mathscr{N}_1 \mathscr{N}_2 \mathscr{N}_3 e^{\mathscr{N}_3 m_3^{-1} t}}{I_3 I_1 - (I_1 \mathscr{U}_1 \mathscr{N}_2 \mathscr{N}_3 e^{\mathscr{N}_1 m_1^{-1} t} + I_2 \mathscr{U}_2 \mathscr{N}_1 \mathscr{N}_3 e^{\mathscr{N}_2 m_2^{-1} t} + I_1 I_2 \mathscr{U}_3 \mathscr{N}_1 \mathscr{N}_2 e^{\mathscr{N}_3 m_3^{-1} t})} \right).
\end{aligned}
\tag{4.10}
$$

In the spirit of transparency, observe that we have just set:

$$
\begin{gathered}
\mathscr{N}_1 m_1^{-1} = -\nu_{18}^f k_{f_8}, \quad \mathscr{N}_2 m_2^{-1} = -\nu_{29}^f k_{f_9}, \quad \mathscr{N}_3 m_3^{-1} = -\nu_{310}^f k_{f_{10}}, \\
\mathscr{U}_1 m_1^{-1} = k_{f_3}[\mathfrak{N}_1], \quad \mathscr{O}_{21} m_2^{-1} = k_{f_1}, \quad \mathscr{O}_{31} m_3^{-1} = (2k_{f_2} - k_{f_6}), \\
\mathscr{O}_{12} m_1^{-1} = -k_{f_1}, \quad \mathscr{U}_2 m_2^{-1} = -k_{f_5}[\mathfrak{N}_3], \quad \mathscr{O}_{32} m_3^{-1} = -k_{f_4}[\mathfrak{N}_2], \\
\mathscr{O}_{13} m_1^{-1} = (2k_{f_6} - k_{f_2}), \quad \mathscr{O}_{23} m_2^{-1} = k_{f_4}[\mathfrak{N}_2], \quad \mathscr{U}_3 m_3^{-1} = k_{f_7}[\mathfrak{N}_5],
\end{gathered}
$$

where to satisfy the first set of constraints we set, $k_{f_1} = 1/2$, $k_{f_2} = 1$, $k_{f_3} = 1/2$, $k_{f_6} = 3/2$ and $[\mathfrak{N}_1] = 1$. The second set of constraints are satisfied by setting, $k_{f_5} = 1/2$, $k_{f_4} = 1/2$, $[\mathfrak{N}_3] = 1$, and $[\mathfrak{N}_2] = 1$. And by consistency the third set of constraints then become, $k_{f_7} = 1/2$ and $[\mathfrak{N}_5] = 1$, which yields for the first set that: $\mathscr{N}_1 = -\nu_{18}^f k_{f_8}, \mathscr{N}_2 = -\nu_{29}^f k_{f_9}, \mathscr{N}_3 = -\nu_{310}^f k_{f_{10}}$. We choose the remaining variables as $\nu_{18}^f = \nu_{29}^f = \nu_{310}^f = 1$, and $k_{f_8} = \frac{1}{2} n_{1,0}$, $k_{f_9} = \frac{1}{2} n_{2,0}$, and $k_{f_{10}} = \frac{1}{2} n_{3,0}$.

Finally we set the initial state of the coupled system. Consider the function,

$$
\chi = \beta + \sin \boldsymbol{x} + \sin(\beta^{N-2} y) + \cos(\beta^{N-2} x),
$$

letting $\beta \in \mathbb{R}$ and where $\boldsymbol{x} = (xy)$ when $N = 2$ and $\boldsymbol{x} = (xyz)$ when $N = 3$. Then the initial conditions are simply chosen to satisfy $\rho_i = \beta^{-3} \chi^3$, where for simplicity we fix $\beta = 10$. The timestepping is chosen in each case to avoid stability related errors, such that $\Delta t = 0.01$ seconds.

Let us briefly discuss the convergence results here, as shown in Figures 4–6, and Tables 2–4. As prescribed we achieve the expected convergence rates in h, which converge rapidly to $p + 1$ in any N (we do not show dimension one for the sake of space). Similarly we see the linear behavior of the p-convergence in the proper norm, though at a faster rate than the h convergence. It is interesting to note that this seems to indicate that p-enrichment might be more suitable than h-refinement, when one must be chosen over the other. However, we caution that this behavior seems to be fairly problem dependent and may not easily generalize.

§4.2.2 **Mass diffusion and *hp*-adaptivity**

Finally let us consider the full system (4.7), with nonzero mass diffusion. In this case, the nonzero diffusive fluxes drive entropic jumps across the cell boundaries which, as discussed in §3.3, can be used to elicit an h-adaptivity strategy. Here we take the same system as presented in §4.2.1 yet couple to it a diagonal matrix $\mathscr{D}_i$ with homogeneous entries of 1×10^{-4} m^2/s. We choose this representation to avoid the complications arising in §2.5 for a choice of nonconstant mass diffusivity, since this choice does not very strongly affect the behavior in the coupled entropy functions.

Here again, we set the same initial conditions from §4.2.1, given the same timestepping, yet we find because the coefficients in the first integrals of the exact solution (4.10) depend on our choice of initial conditions (by construction), then we no longer have a decoupled time-dependent solution to the mass action. Namely, (4.10) is not a solution to the initial value nFANODE problem with the mass diffusion turned on in this instance, as the diffusion alters the subsequent initial state of the system at each subsequent timestep.

As a consequence we arrive at a system that has no exact representation, and thus we measure the relative error with respect to a top degree polynomial at maximum refinement. The mass diffusion here leads to substantial boundary layer formation along $\partial\Omega_{hp}$. These boundary layers, it turns out, end up dominating the entropy formation in the solution, particularly the entropic jumps (see the large boundary layer behavior in the

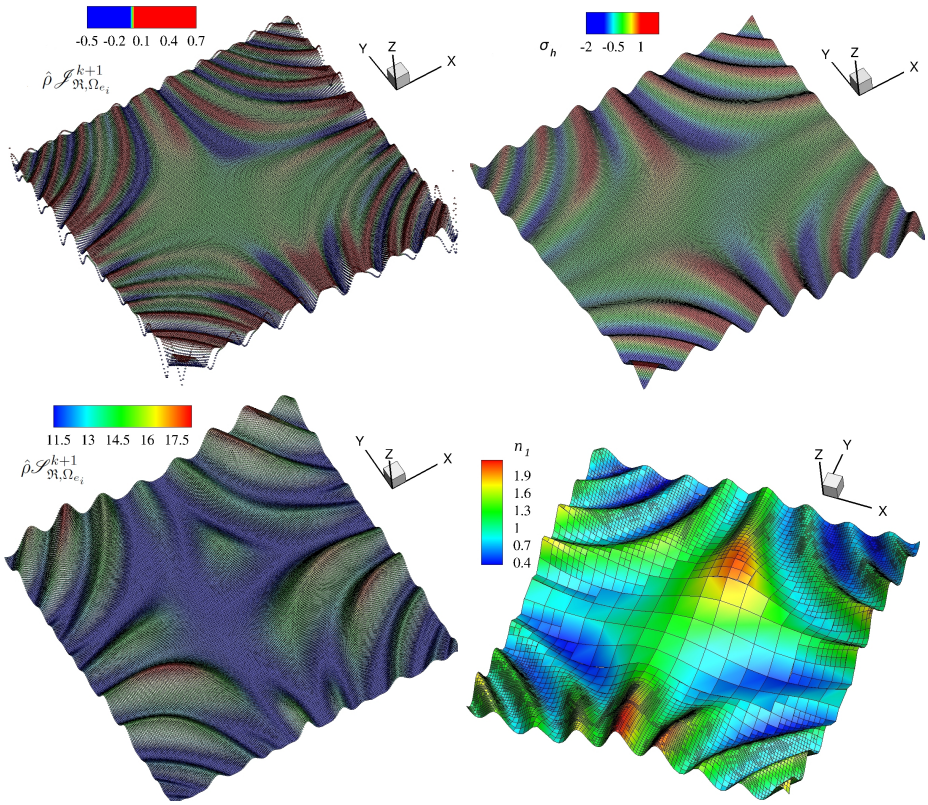

Figure 7: Here we show the derived variables of our solutions from §4.2.2, as well as an example of the h-refinement scheme that emerges. The upper left is the density of the entropic jump (with prevalent boundary layer), the top right is the gradient of the solution, and the bottom left is the entropy density, each evaluated at timestep five using $\Delta t = 0.01$ with hp-adaptation turned off, and $h = 1/256$. On the bottom right is an example of the h-refinement scheme that emerges from §4.2.2 after eleven timesteps of $\Delta t = 0.01$, where we have a Type I refinement scheme for h and a Type II enrichment scheme for p. The limits are $\iota_s = 0.2$ and $\iota_h = 0.05$, with $h \in \{1/16, 1/32, 1/64, 1/128, 1/256\}$ and $p = \{1, 2, 3\}$.

	IMEX L^2-error			RKC, $\epsilon = 2/13$, L^2-error			RKSSP(2,2), L^2-error		
h	$p=1$	$p=2$	$p=3$	$p=1$	$p=2$	$p=3$	$p=1$	$p=2$	$p=3$
$\frac{1}{256}$	0.00287	0.00021	–	0.00190	0.00024	–	0.00217	0.00067	–
$\frac{1}{128}$	0.01147	0.00049	0.00022	0.00759	0.00042	0.00027	0.00748	0.00139	0.00076
$\frac{1}{64}$	0.04564	0.00315	0.00036	0.03029	0.00186	0.00037	0.02973	0.00277	0.00151
$\frac{1}{32}$	0.17519	0.02513	0.00285	0.11865	0.01412	0.00149	0.11723	0.01422	0.00261
$\frac{1}{16}$	0.70421	0.14438	0.04851	0.46633	0.09193	0.02279	0.46165	0.09129	0.02281

Table 5: We give the L^2-errors for the h and p ramping along the LV solution with homogeneous diffusion added (i.e. substantial boundary layers present). Here we have set $\Delta t = 0.01$ seconds, and $T = 0.5$ s.

entropic jumps, which is not present in the gradient in 7) that drive the h-adaptation. Though this layer is not in general of definite sign (in the entropic flux), one might surmise that switching simply between Type I and Type II methods, as discussed in §3, should appropriately solve this issue, selecting the lower center cells for refinement, while letting the boundary layer "smear out." However, this point broaches the central nuance of hp-adaptive dioristic schemes.

This system, which is inherently more physical than our previous cases, now demonstrates a complicated

	IMEX L^2-error			RKC, $\epsilon = 2/13$, L^2-error			RKSSP(2,2), L^2-error		
h	$p=1$	$p=2$	$p=3$	$p=1$	$p=2$	$p=3$	$p=1$	$p=2$	$p=3$
1/64	0.00026	4.6e-06	–	0.00033	5.4e-06	–	0.00026	4.6e-06	–
1/32	0.00084	3.1e-05	1.4e-06	0.00106	3.9e-05	1.4e-06	0.00084	3.1e-05	1.4e-06
1/16	0.00173	0.00031	1.9e-05	0.00219	0.00039	2.4e-05	0.00173	0.00031	1.9e-05
hp	$\iota_s = \iota_h = 0.5$, 2.7e-06			$\iota_s = \iota_h = 0.5$, 3.3e-06			$\iota_s = \iota_h = 0.5$, 2.7e-06		

Table 6: We give the L^2-errors for the h and p ramping of the equilibrium solution with homogeneous diffusion added. Here we have set $\Delta t = 0.01$ seconds, and $T = 0.5$ s. The p-enrichment scheme is of Type II and the h-adaptive scheme is of Type I, and both span all h and p levels (*i.e.* $p \in \{1, 2, 3\}$ $h \in \{1/16, 1/32, 1/64\}$).

entropic response surface that can not only drive the hp-adaptivity, but reveals a number of subtle characteristics in the physics of the solutions space. Notice for example in Figure 7 that the entropy behavior is substantially different than that of the solution gradient, which is what most standard hp-adaptive schemes use to drive the adaptivity.

Let us emphasize this numerical observation for the interested reader. In a dioristic scheme — in fact, in any hp-adaptation scheme that does not rely on an *a posteriori* minimization technique — one sees a spike in the entropy around the points (i.e. quadrature points) of adaptation, whether they be points that have been p-adapted or h-adapted (in either direction, e.g. higher or lower levels). These spikes are easily observed by the highly nonlinear entropy functionals, but are only very small oscillatory perturbations in the solution itself. This behavior is seen in Figure 7, where one cannot see the spikes in the solution and its gradient, but the nonlinear entropic jump clearly show the anomalous behavior at the domain boundary. Moreover, these spikes in the entropy will in general equilibrate over some characteristic time t^w, depending on the dynamics of the solutions space. However, if t^w is not achieved, then the local perturbations get amplified by the h or p adaptations, and lead to either cascading instabilities or a slow increase in the total energy of the solution (which can be quantified in the error). This behavior has been observed before [58, 60] in different contexts. In general identifying t^w is, at this point, simply an empirical process that can be informed by CFL-type stability relations for reaction-diffusion problems.

However, in the presence of strong boundary layers these local perturbations are also amplified by the boundary layer effects, leading to rather stringent restrictions on the t^w, which substantially reduce the robustness of the dioristic entropy scheme in the presence of dominating boundary layers for reaction–diffusion problems, as demonstrated in Table 5. On the other hand, when this is not the case and the domain boundary entropy does not dictate the behavior of the entropic growth of the solution, then the hp-adaptation scheme from §3 is extremely robust. For example, consider our equilibrium problem from §4.1, where we again add a simple homogeneous diffusion $\mathscr{D}_i$ of 1×10^{-4} m^2/s. Then, as seen in Table 6, the convergence in the hp setting is very robust and remarkably easy to achieve.

§5 Conclusion

We have developed from first principles a family of reaction–diffusion equations that obey equation ordering. We denote this restricted family as *quiescent reactors*, in order to elicit the concept of "quiescent reactors" from the experimental sciences where "dampened stirring effects" are the subject of study. In section §2 we derive the system from the species Boltzmann equations, where a number of approximate constraints dictate the relevance and appropriateness of the model regime to a particular application model. Operator splitting strategies between the *mass diffusion* component and a *mass action* component lead to a nonlinear system of ODEs coupled to parabolic PDEs, allowing the utilization of powerful mathematical tools in approaching the numerical solution methods.

In §2.6–2.7 we discuss in detail the numerical methods at play in the paper. Generally this reduces to a mixed form discontinuous Galerkin spatial discretization approach with mixed form (implicit and/or explicit) temporal discretization strategies that recover multiscale effects. This discretization couples in §3 to a novel entropy/stability result that emerges from the regularity analysis of the base equations (2.11). The entropy

functional is then used as a consistency measure on the numerics of the solution, as well as a driving parameter for a *dioristic entropy hp*-adaptivity strategy.

This mixed-form discontinuous Galerkin local IMEX stability preserving split operator dioristic-entropic *hp*-adaptive scheme is applied to a number of numerical examples in §4. These methods achieve optimal convergence results in both h and p, and further recover exponential convergence results of general *hp*-adaptive strategies as long as domain boundary layers do not dominate the entropy formation. This is remarkable in that the usual observation of mixing error polluting convergence rates seems to be largely absent when perfoming the *hp*-adaptivity using the mathematically rigorous entropic formulation.

Our future directions are to extend the quiescent reactors to include fluid reactors where density $\rho = \rho(t, \boldsymbol{x})$ and temperature (energy) $\mathfrak{E} = \mathfrak{E}(\vartheta) = \mathfrak{E}(\vartheta(t, \boldsymbol{x}))$ are fully coupled, in addition to adding turbulence models and electromagnetic fields for weakly ionized and plasma reactors. This includes extending the results similar to herein to convection dominated multicomponent systems of convection–reaction–diffusion equations Such systems include the multicomponent reactive Euler equations, the multicomponent reactive Navier–Stokes equations, and the multicomponent reactive magnetohydrodynamic equations, as well as more general multicomponent reactive magnetofluid systems.

References

[1] B. V. Alexeev, A. Chikhaoui, and I. T. Grushin. Application of the generalized chapman-enskog method to the transport-coefficient calculation in a reacting gas mixture. *Phys. Rev. E*, 49(4):2809–2825, Apr 1994.

[2] D. Arnold, F. Brezzi, B. Cockburn, and D. Marini. Discontinuous Galerkin methods for elliptic problems. In *Discontinuous Galerkin methods (Newport, RI, 1999)*, volume 11 of *Lect. Notes Comput. Sci. Eng.*, pages 89–101. Springer, Berlin, 2000.

[3] D. N. Arnold, F. Brezzi, B. Cockburn, and L. D. Marini. Unified analysis of discontinuous Galerkin methods for elliptic problems. *SIAM J. Numer. Anal.*, 39(5):1749–1779, 2001/02.

[4] P. J. Atzberger. Spatially adaptive stochastic numerical methods for intrinsic fluctuations in reaction-diffusion systems. *Journal of Computational Physics*, 229(9):3474 – 3501, 2010.

[5] O. Babelon, D. Bernard, and M. Talon. *Introduction to classical integrable systems*. Cambridge Monographs on Mathematical Physics. Cambridge University Press, Cambridge, 2003.

[6] W. Bangerth, R. Hartmann, and G. Kanschat. deal.II – a general purpose object oriented finite element library. *ACM Trans. Math. Softw.*, 33(4):24/1–24/27, 2007.

[7] W. Bangerth and O. Kayser-Herold. Data structures and requirements for hp finite element software. *ACM Trans. Math. Softw.*, 36:4:1–4:31, March 2009.

[8] C. Baumann and J. Oden. A discontinuous *hp* finite element method for convection-diffusion problems. *Computer Methods in Applied Mechanics and Engineering*, 175(3-4):311–341, JUL 2 1999.

[9] M. Bendahmane, R. Bürger, R. Ruiz-Baier, and K. Schneider. Adaptive multiresolution schemes with local time stepping for two-dimensional degenerate reaction-diffusion systems. *Appl. Numer. Math.*, 59(7):1668–1692, 2009.

[10] M. Bergdorf, I. Sbalzarini, and P. Koumoutsakos. A lagrangian particle method for reaction-diffusion systems on deforming surfaces. *Journal of Mathematical Biology*, 61:649–663, 2010. 10.1007/s00285-009-0315-2.

[11] M. Bisi and L. Desvillettes. From reactive Boltzmann equations to reaction-diffusion systems. *J. Stat. Phys.*, 124(2-4):881–912, 2006.

[12] G. W. Bluman and S. C. Anco. *Symmetry and integration methods for differential equations*, volume 154 of *Applied Mathematical Sciences*. Springer-Verlag, New York, 2002.

[13] D. Bothe and M. Pierre. Quasi-steady-state approximation for a reaction-diffusion system with fast intermediate. *J. Math. Anal. Appl.*, 368(1):120–132, 2010.

[14] L. Brenig. Complete factorisation and analytic solutions of generalized lotka-volterra equations. *Physics Letters A*, 133(7-8):378 – 382, 1988.

[15] L. Brenig and A. Goriely. Universal canonical forms for time-continuous dynamical systems. *Phys. Rev. A*, 40(7):4119–4122, Oct 1989.

[16] P. N. Brown and Y. Saad. Convergence theory of nonlinear Newton-Krylov algorithms. *SIAM J. Optim.*, 4(2):297–330, 1994.

[17] L. Cairó. Darboux first integral conditions and integrability of the 3D Lotka-Volterra system. *J. Nonlinear Math. Phys.*, 7(4):511–531, 2000.

[18] M. C. Caputo and A. Vasseur. Global regularity of solutions to systems of reaction-diffusion with sub-quadratic growth in any dimension. *Comm. Partial Differential Equations*, 34(10-12):1228–1250, 2009.

[19] C. Cercignani. *The Boltzmann equation and its applications*, volume 67 of *Applied Mathematical Sciences*. Springer-Verlag, New York, 1988.

[20] V. K. Chandrasekar, M. Senthilvelan, and M. Lakshmanan. On the complete integrability and linearization of nonlinear ordinary differential equations. III. Coupled first-order equations. *Proc. R. Soc. Lond. Ser. A Math. Phys. Eng. Sci.*, 465(2102):585–608, 2009.

[21] S. Chapman and T. G. Cowling. *The mathematical theory of nonuniform gases*. Cambridge Mathematical Library. Cambridge University Press, Cambridge, third edition, 1990. An account of the kinetic theory of viscosity, thermal conduction and diffusion in gases, In co-operation with D. Burnett, With a foreword by Carlo Cercignani.

[22] E. S. Cheb-Terrab, L. G. S. Duarte, and L. A. C. P. da Mota. Computer algebra solving of first order ODEs using symmetry methods. *Comput. Phys. Comm.*, 101(3):254–268, 1997.

[23] H. P. Cheng, G. T. Yeh, and J. R. Cheng. A numerical model simulating reactive transport in shallow water domains: model development and demonstrative applications. *Advances in Environmental Research*, 4(3):187 – 209, 2000.

[24] C. N. Dawson, H. Klíe, M. F. Wheeler, and C. S. Woodward. A parallel, implicit, cell-centered method for two-phase flow with a preconditioned Newton-Krylov solver. *Comput. Geosci.*, 1(3-4):215–249 (1998), 1997.

[25] L. Demkowicz. *Computing with hp-adaptive finite elements. Vol. 1.* Chapman & Hall/CRC Applied Mathematics and Nonlinear Science Series. Chapman & Hall/CRC, Boca Raton, FL, 2007. One and two dimensional elliptic and Maxwell problems, With 1 CD-ROM (UNIX).

[26] L. Demkowicz. A new discontinuous Petrov-Galerkin method with optimal test functions. part v: Solution of 1d burgers' and navier-stokes equations. page 34, 2010.

[27] L. Demkowicz and J. Gopalakrishnan. A class of discontinuous Petrov-Galerkin methods. Part I: the transport equation. *Comput. Methods Appl. Mech. Engrg.*, 199(23-24):1558–1572, 2010.

[28] C. V. den Broeck, J. Houard, and M. M. Mansour. Chapman-Enskog development of the multivariate master equation. *Physica A: Statistical and Theoretical Physics*, 101(1):167 – 184, 1980.

[29] S. Descombes, T. Dumont, V. Louvet, and M. Massot. On the local and global errors of splitting approximations of reaction-diffusion equations with high spatial gradients. *Int. J. Comput. Math.*, 84(6):749–765, 2007.

[30] S. Descombes and M. Massot. Operator splitting for nonlinear reaction-diffusion systems with an entropic structure: singular perturbation and order reduction. *Numer. Math.*, 97(4):667–698, 2004.

[31] L. Desvillettes, R. Monaco, and F. Salvarani. A kinetic model allowing to obtain the energy law of polytropic gases in the presence of chemical reactions. *European Journal of Mechanics - B/Fluids*, 24(2):219 – 236, 2005.

[32] L. G. S. Duarte, S. E. S. Duarte, and L. A. C. P. da Mota. A method to tackle first-order ordinary differential equations with Liouvillian functions in the solution. *J. Phys. A*, 35(17):3899–3910, 2002.

[33] L. G. S. Duarte, S. E. S. Duarte, L. A. C. P. da Mota, and J. E. F. Skea. An extension of the Prelle-Singer method and a Maple implementation. *Comput. Phys. Comm.*, 144(1):46–62, 2002.

[34] P. Érdi and J. J. Tóth. *Mathematical models of chemical reactions : theory and applications of deterministic and stochastic models*. Princeton University Press. Cambridge University Press, Princeton, N.J., third edition, 1989. An account of the kinetic theory of viscosity, thermal conduction and diffusion in gases, In co-operation with D. Burnett, With a foreword by Carlo Cercignani.

[35] A. Ern and V. Giovangigli. *Multicomponent transport algorithms*, volume 24 of *Lecture Notes in Physics. New Series m: Monographs*. Springer-Verlag, Berlin, 1994.

[36] A. Ern and V. Giovangigli. The kinetic chemical equilibrium regime. *Physica A: Statistical and Theoretical Physics*, 260(1-2):49 – 72, 1998.

[37] L. Ferm, A. Hellander, and P. Lötstedt. An adaptive algorithm for simulation of stochastic reaction-diffusion processes. *J. Comput. Phys.*, 229(2):343–360, 2010.

[38] J. Ferris, B. Tran, J. Joseph, V. Vuitton, R. Briggs, and M. Force. The role of photochemistry in titan's atmospheric chemistry. *Advances in Space Research*, 36(2):251 – 257, 2005. Space Life Sciences: Astrobiology: Steps toward Origin of Life and Titan before Cassini.

[39] W. Gardiner. *Combustion Chemistry*. Springer-Verlag New York Inc., New York, NY, 1984.

[40] V. Giovangigli. *Multicomponent flow modeling*. Modeling and Simulation in Science, Engineering and Technology. Birkhäuser Boston Inc., Boston, MA, 1999.

[41] V. Giovangigli and M. Massot. Entropic structure of multicomponent reactive flows with partial equilibrium reduced chemistry. *Math. Methods Appl. Sci.*, 27(7):739–768, 2004.

[42] A. Goriely. *Integrability and nonintegrability of dynamical systems*, volume 19 of *Advanced Series in Nonlinear Dynamics*. World Scientific Publishing Co. Inc., River Edge, NJ, 2001.

[43] S. Gottlieb, C.-W. Shu, and E. Tadmor. Strong stability-preserving high-order time discretization methods. *SIAM Rev.*, 43(1):89–112 (electronic), 2001.

[44] T. Goudon and A. Vasseur. Regularity analysis for systems of reaction-diffusion equations. *Ann. Sci. Éc. Norm. Supér. (4)*, 43(1):117–142, 2010.

[45] M. Groppi, A. Rossani, and G. Spiga. Kinetic theory of a diatomic gas with reactions of dissociation and recombination through a transition state. *Journal of Physics A: Mathematical and General*, 33(48):8819, 2000.

[46] B. Hernández-Bermejo and V. Fairén. Lotka-volterra representation of general nonlinear systems. *Mathematical Biosciences*, 140(1):1 – 32, 1997.

[47] J. Hirschfelder, C. Curtiss, and R. Bird. *The Molecular Theory of Gases and Liquids*. Structure of Matter Series. Wiley-Interscience, Revised, New York, 1954.

[48] P. E. Hydon. *Symmetry methods for differential equations*. Cambridge Texts in Applied Mathematics. Cambridge University Press, Cambridge, 2000. A beginner's guide.

[49] F. Ilinca and J.-F. Hétu. A new stabilized finite element method for reaction-diffusion problems: the source-stabilized Petrov-Galerkin method. *Internat. J. Numer. Methods Engrg.*, 75(13):1607–1630, 2008.

[50] S. A. Isaacson. Relationship between the reaction-diffusion master equation and particle tracking models. *J. Phys. A*, 41(6):065003, 15, 2008.

[51] S. A. Isaacson. The reaction-diffusion master equation as an asymptotic approximation of diffusion to a small target. *SIAM J. Appl. Math.*, 70(1):77–111, 2009.

[52] S. A. Isaacson. The reaction-diffusion master equation as an asymptotic approximation of diffusion to a small target. *SIAM J. Appl. Math.*, 70(1):77–111, 2009.

[53] S. Jagannathan, J. S. Dahler, and W. Sung. Nonequilibrium phenomena in dense polyatomic fluids. i. transport coefficients for axially symmetric (polar) molecules. *Journal of Chemical Physics*, 83(4):1808–1821, 1985.

[54] G. Kanschat. Multilevel methods for discontinuous Galerkin FEM on locally refined meshes. *Computers & Structures*, 82(28):2437 – 2445, 2004. Preconditioning methods: algorithms, applications and software environments.

[55] D. E. Keyes, D. R. Reynolds, and C. S. Woodward. Implicit solvers for large-scale nonlinear problems. *J. Phys. Conf. Ser.*, 46:433–442, 2006. SciDAC 2006, Scientific discovery through advanced computing.

[56] X. Liu and Q. Nie. Compact integration factor methods for complex domains and adaptive mesh refinement. *J. Comput. Phys.*, 229(16):5692–5706, 2010.

[57] J. M. Melenk and C. Schwab. *HP* FEM for reaction-diffusion equations. I. Robust exponential convergence. *SIAM J. Numer. Anal.*, 35(4):1520–1557 (electronic), 1998.

[58] C. Michoski, C. Dawson, E. Kubatko, C. Mirabito, J. Westerink, and D. Wirasaet. Dynamic p-enrichment schemes for multicomponent reactive flows. *Advances in Water Resources*, *In press*, 2011.

[59] C. Michoski, J. A. Evans, P. G. Schmitz, and A. Vasseur. A discontinuous Galerkin method for viscous compressible multifluids. *J. Comput. Phys.*, 229(6):2249–2266, 2010.

[60] C. Michoski, C. Mirabito, C. Dawson, E. Kubatko, D. Wirasaet, and J. Westerlink. Adaptive hierarchic transformations over dynamic p-enriched schemes applied to generalized DG systems. *J. Comput. Phys.*, *submitted*, 2010.

[61] C. Michoski and A. Vasseur. Existence and uniqueness of strong solutions for a compressible multiphase navier-stokes miscible fluid-flow problem in dimension n=1. *Math. Models Methods Appl. Sci.*, In Press, 2008.

[62] D. J. Miller and A. Ghosh. A fully adaptive reaction-diffusion integration scheme with applications to systems biology. *Journal of Computational Physics*, 226(2):1509 – 1531, 2007.

[63] J. Moulin Ollagnier. Algorithms and methods in differential algebra. *Theoret. Comput. Sci.*, 157(1):115–127, 1996. Algorithmic complexity of algebraic and geometric models (Creteil, 1994).

[64] J. T. Oden, I. Babuška, and C. E. Baumann. A discontinuous *hp* finite element method for diffusion problems. *J. Comput. Phys.*, 146(2):491–519, 1998.

[65] P. J. Olver. *Applications of Lie groups to differential equations*, volume 107 of *Graduate Texts in Mathematics*. Springer-Verlag, New York, second edition, 1993.

[66] W. Pang, W. Xu, C. Sun, C. Zhang, and G. Chen. Methane hydrate dissociation experiment in a middle-sized quiescent reactor using thermal method. *Fuel*, 88(3):497 – 503, 2009.

[67] A. Paster, D. Bolster, and D. A. Benson. Connecting the dots: Semi-analytical and random walk numerical solutions of the diffusion-reaction equation with stochastic initial conditions. *Journal of Computational Physics*, 263(0):91 – 112, 2014.

[68] R. R. Pompano, H.-W. Li, and R. F. Ismagilov. Rate of mixing controls rate and outcome of autocatalytic processes: Theory and microfluidic experiments with chemical reactions and blood coagulation. *Biophysical Journal*, 95(3):1531 – 1543, 2008.

[69] J. Powell and M. Tabor. Nongeneric connections corresponding to front solutions. *J. Phys. A*, 25(13):3773–3796, 1992.

[70] M. J. Prelle and M. F. Singer. Elementary first integrals of differential equations. *Trans. Amer. Math. Soc.*, 279(1):215–229, 1983.

[71] D. L. Ropp and J. N. Shadid. Stability of operator splitting methods for systems with indefinite operators: reaction-diffusion systems. *J. Comput. Phys.*, 203(2):449–466, 2005.

[72] O. Roussel, K. Schneider, A. Tsigulin, and H. Bockhorn. A conservative fully adaptive multiresolution algorithm for parabolic PDEs. *J. Comput. Phys.*, 188(2):493–523, 2003.

[73] S. J. Ruuth. Global optimization of explicit strong-stability-preserving Runge-Kutta methods. *Math. Comp.*, 75(253):183–207 (electronic), 2006.

[74] R. Sandboge. Adaptive finite element methods for systems of reaction-diffusion equations. *Comput. Methods Appl. Mech. Engrg.*, 166(3-4):309–328, 1998.

[75] C.-W. Shu and S. Osher. Efficient implementation of essentially nonoscillatory shock-capturing schemes. *J. Comput. Phys.*, 77(2):439–471, 1988.

[76] J. Smoller. *Shock waves and reaction-diffusion equations*, volume 258 of *Grundlehren der Mathematischen Wissenschaften [Fundamental Principles of Mathematical Sciences]*. Springer-Verlag, New York, second edition, 1994.

[77] V. N. Snytnikov, G. I. Dudnikova, J. T. Gleaves, S. A. Nikitin, V. N. Parmon, V. O. Stoyanovsky, V. A. Vshivkov, G. S. Yablonsky, and V. S. Zakharenko. Space chemical reactor of protoplanetary disk. *Advances in Space Research*, 30(6):1461 – 1467, 2002.

[78] B. Sportisse. An analysis of operator splitting techniques in the stiff case. *J. Comput. Phys.*, 161(1):140–168, 2000.

[79] G. Strang. On the construction and comparison of difference schemes. *SIAM J. Numer. Anal.*, 5:506–517, 1968.

[80] S. M. Suh, M. R. Zachariah, and S. L. Girshick. Numerical modeling of silicon oxide particle formation and transport in a one-dimensional low-pressure chemical vapor deposition reactor. *Journal of Aerosol Science*, 33(6):943 – 959, 2002.

[81] J. Sutherland and C. Kennedy. Improved boundary conditions for viscous, reacting, compressible flows. *J. Comput. Phys.*, 191:502–524, 2003.

[82] M. Suzuki. General theory of fractal path integrals with applications to many-body theories and statistical physics. *J. Math. Phys.*, 32(2):400–407, 1991.

[83] M. Torrilhon and R. Jeltsch. Essentially optimal explicit Runge-Kutta methods with application to hyperbolic-parabolic equations. *Numer. Math.*, 106(2):303–334, 2007.

[84] C. Truesdell and R. Muncaster. *Fundamentals of Maxwell's kinetic theory of a simple monoatomic gas.* Academic Press, New York, 1980.

[85] J. G. Verwer and B. P. Sommeijer. An implicit-explicit Runge-Kutta-Chebyshev scheme for diffusion-reaction equations. *SIAM J. Sci. Comput.*, 25(5):1824–1835 (electronic), 2004.

[86] J. G. Verwer, B. P. Sommeijer, and W. Hundsdorfer. RKC time-stepping for advection-diffusion-reaction problems. *J. Comput. Phys.*, 201(1):61–79, 2004.

[87] Y.-M. Wang. Petrov-Galerkin methods for systems of nonlinear reaction-diffusion equations. *Appl. Math. Comput.*, 96(2-3):209–236, 1998.

[88] C. Xenophontos and L. Oberbroeckling. A numerical study on the finite element solution of singularly perturbed systems of reaction-diffusion problems. *Appl. Math. Comput.*, 187(2):1351–1367, 2007.

[89] C. Xenophontos and L. Oberbroeckling. On the finite element approximation of systems of reaction-diffusion equations by p/hp methods. *J. Comput. Math.*, 28(3):386–400, 2010.

[90] R. Ye, A. Murphy, and T. Ishigaki. Numerical modeling of an Ar-H_2 radio-frequency plasma reactor under thermal and chemical nonequilibrium conditions. *Plasma Chemistry and Plasma Processing*, 27(2):189–204, April 2007.

[91] L. Zhang. Explicit traveling wave solutions of five kinds of nonlinear evolution equations. *J. Math. Anal. Appl.*, 379(1):91–124, 2011.

[92] J. Zhu, Y.-T. Zhang, S. A. Newman, and M. Alber. Application of discontinuous Galerkin methods for reaction-diffusion systems in developmental biology. *J. Sci. Comput.*, 40(1-3):391–418, 2009.